The Effect of Small-Scale Structure on Reionization

Paul R. Shapiro

University of Texas at Austin

KITP, UC Santa Barbara,

September 16, 2004

The Epoch of Reionization

- GP troughs detected in spectra of SDSS quasars at $z > 6$ ==> IGM H I density high enough to suggest reionization only just ended at $z = 6$.

The Epoch of Reionization

- WMAP detection of CMB polarization fluctuations on large angular scale ==> foreground electron scattering optical depth high enough to suggest IGM mostly ionized by z >12.

The Epoch of Reionization

- GP troughs detected in spectra of SDSS quasars at $z > 6$ ==> IGM H I density high enough to suggest reionization only just ended at $z = 6$.
- WMAP detection of CMB polarization fluctuations on large angular scale ==> foreground electron scattering optical depth high enough to suggest IGM mostly ionized by $z > 12$.

The Epoch of Reionization

- GP troughs detected in spectra of SDSS quasars at $z > 6$ ==> IGM H I density high enough to suggest reionization only just ended at $z = 6$.
- WMAP detection of CMB polarization fluctuations on large angular scale ==> foreground electron scattering optical depth high enough to suggest IGM mostly ionized by $z > 12$.
- Plausible explanation: reionization began by $z > 15$ but was extended in time, with final "overlap" of ionized zones at $z = 6$.

Part I: Cosmological Ionization Fronts and the Photoevaporation of Minihalos during Reionization

1. DWARF GALAXY MINIHALOS AT HIGH REDSHIFT

- For ΛCDM, the universe at z > 6 was already filled with dwarf galaxies capable of trapping a piece of the global, intergalactic I-fronts which reionized the universe and photoevaporating their gaseous baryons back into the IGM.

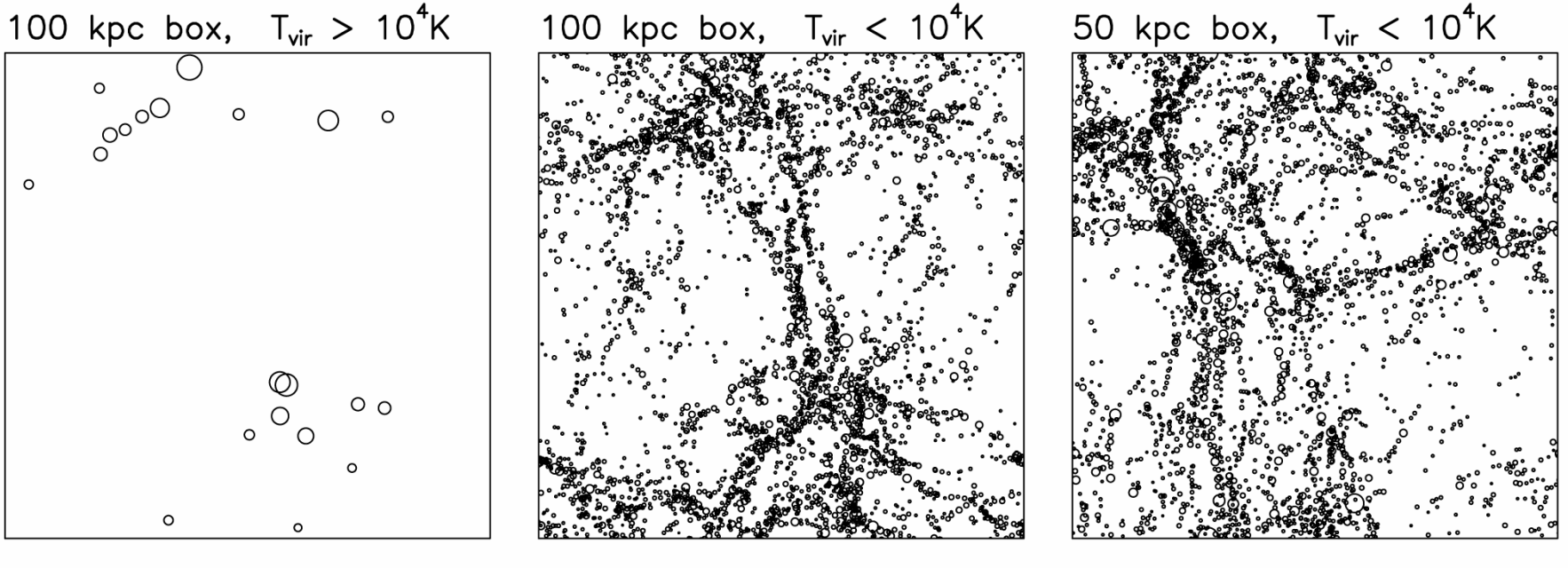

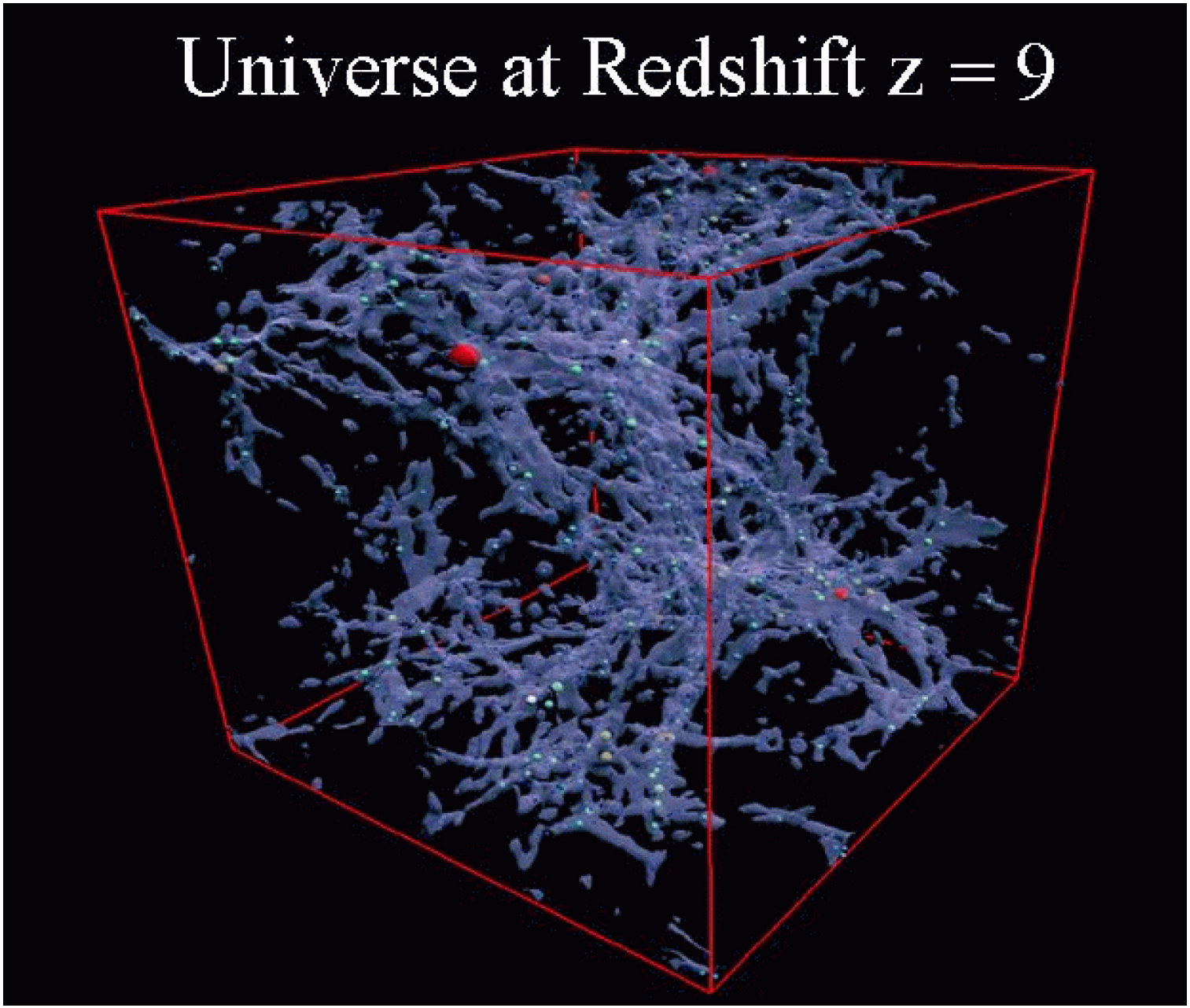
Universe at Redshift z = 9

- Minihalos with $T_{vir} < 10^4$ K were common enough to cover the sky around source halos with $T_{vir} > 10^4$ K during reionization.

ΛCDM HALOS WITHIN 25 KPC AT Z = 9

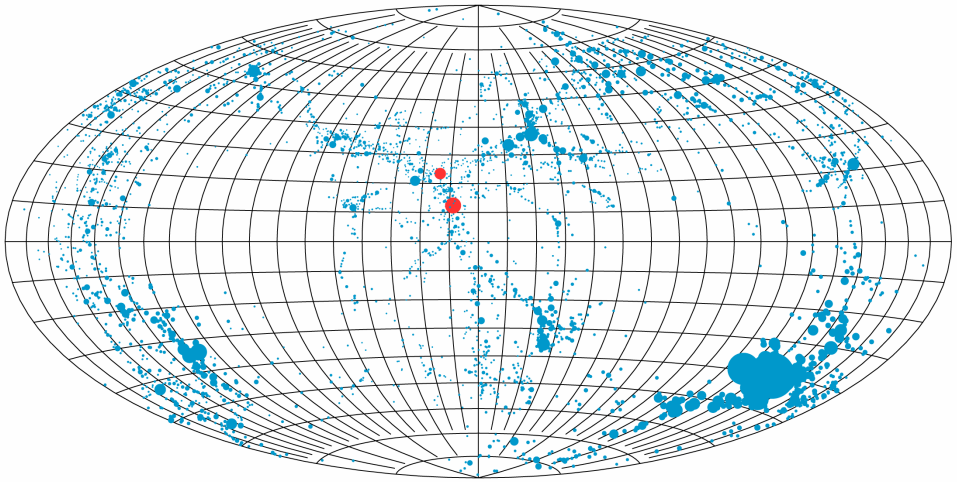

Sky as seen from a random location

Covering fraction : 10.7%

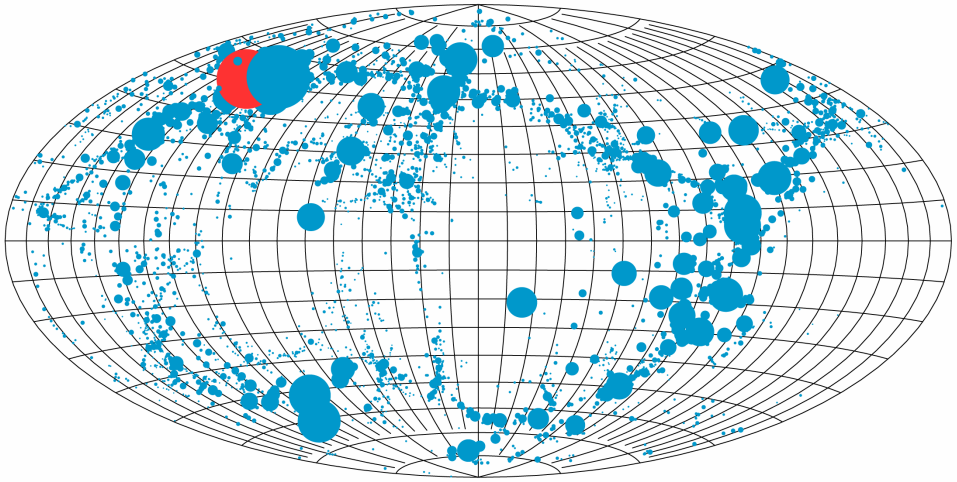

Sky as seen from a 1.1×10^8 $M_\odot$ source

Covering fraction : 23.6%

Fraction of sky covered by minihalos located within the mean volume per source halo, corrected for bias.

- If $M_{source} > 10^8 M_{sun}$, $F_{cover,source} > 1$.

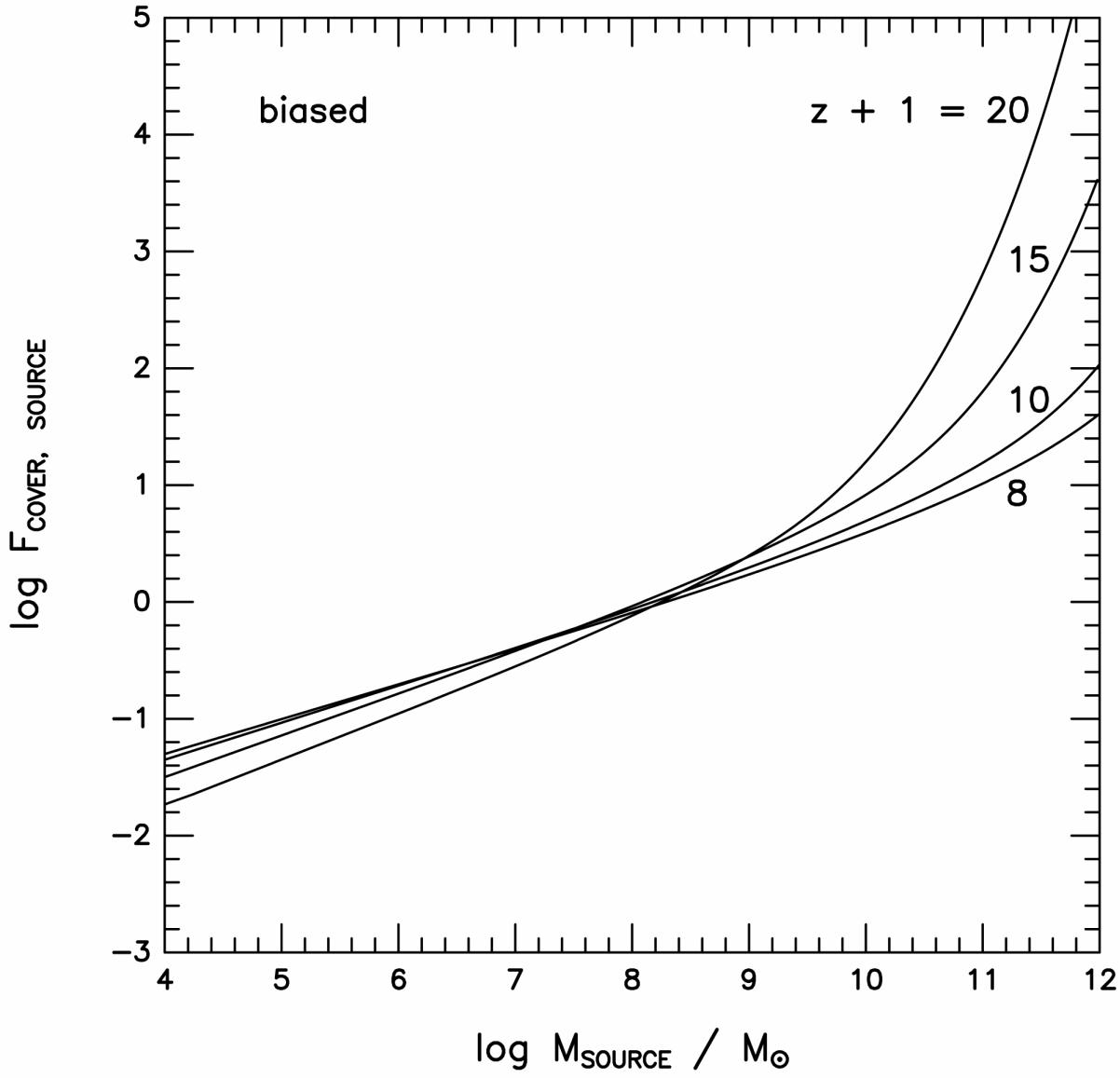

- Photons emitted by any high z source before or during reionization will typically encounter large numbers of photoevaporating minihalos at z > 6.

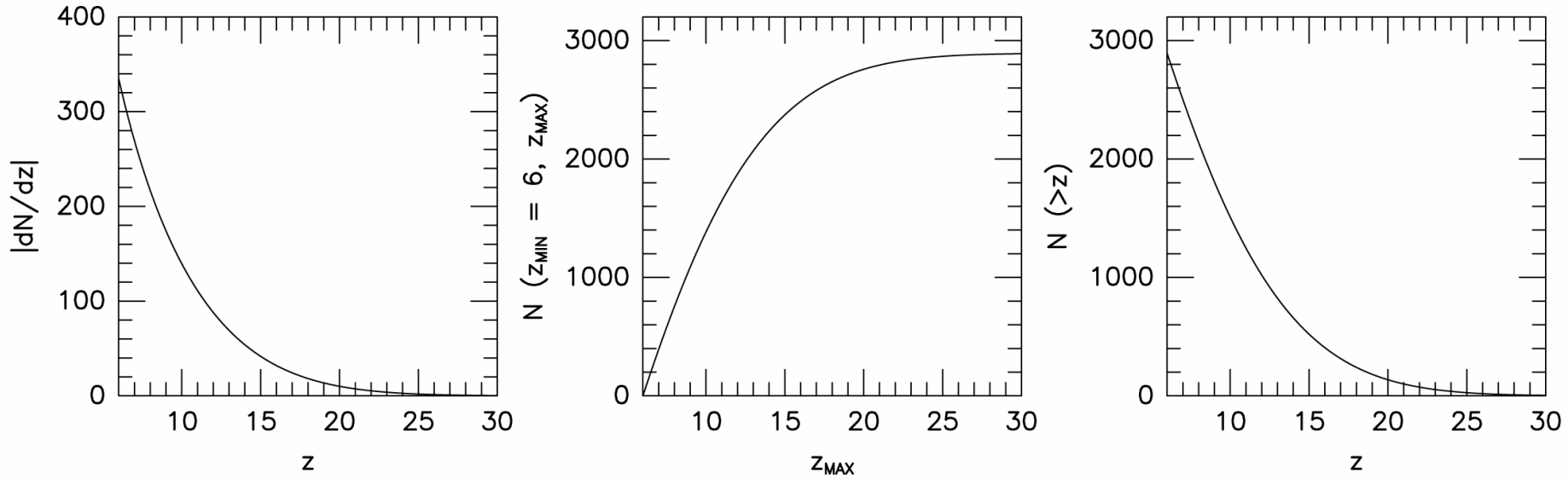

2. THE PHOTOEVAPORATION OF MINIHALOS OVERTAKEN BY COSMOLOGICAL I-FRONTS

(Shapiro, Iliev & Raga 2004)

- We have performed radiation-hydrodynamical simulations of the photoevaporation of a cosmological minihalo overrun by a weak, R-type I-front in the surrounding IGM, created by an external source of radiation.

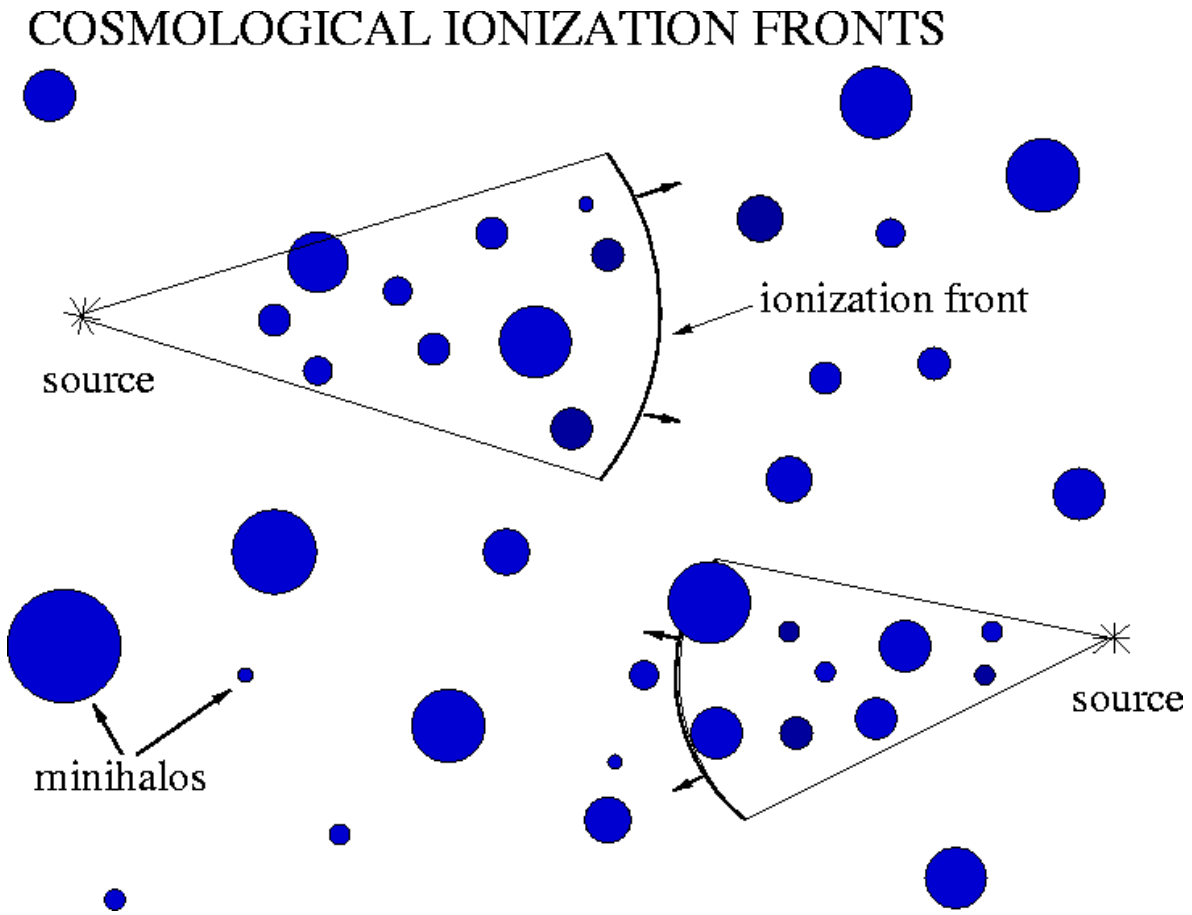

PHOTOEVAPORATION OF MINIHALO DURING COSMOLOGICAL REIONIZATION

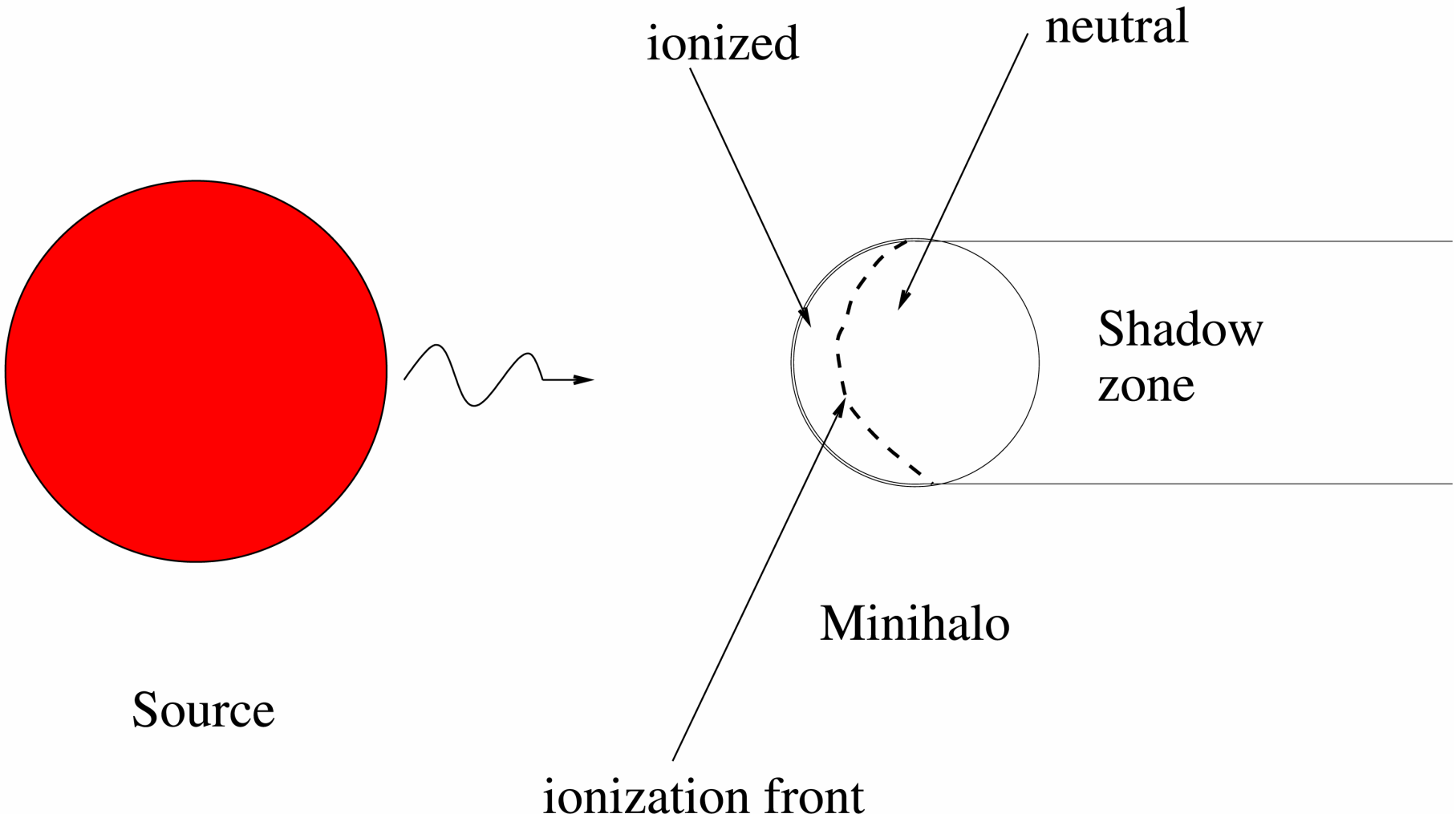

Temperature at times t = 0.0, 0.2, 2.5, 10, 60, 150 Myrs.

(M_{halo}, $z_{initial}$, F_0) = ($10^7 M_{sun}$, 9, 1).

Pop II source.

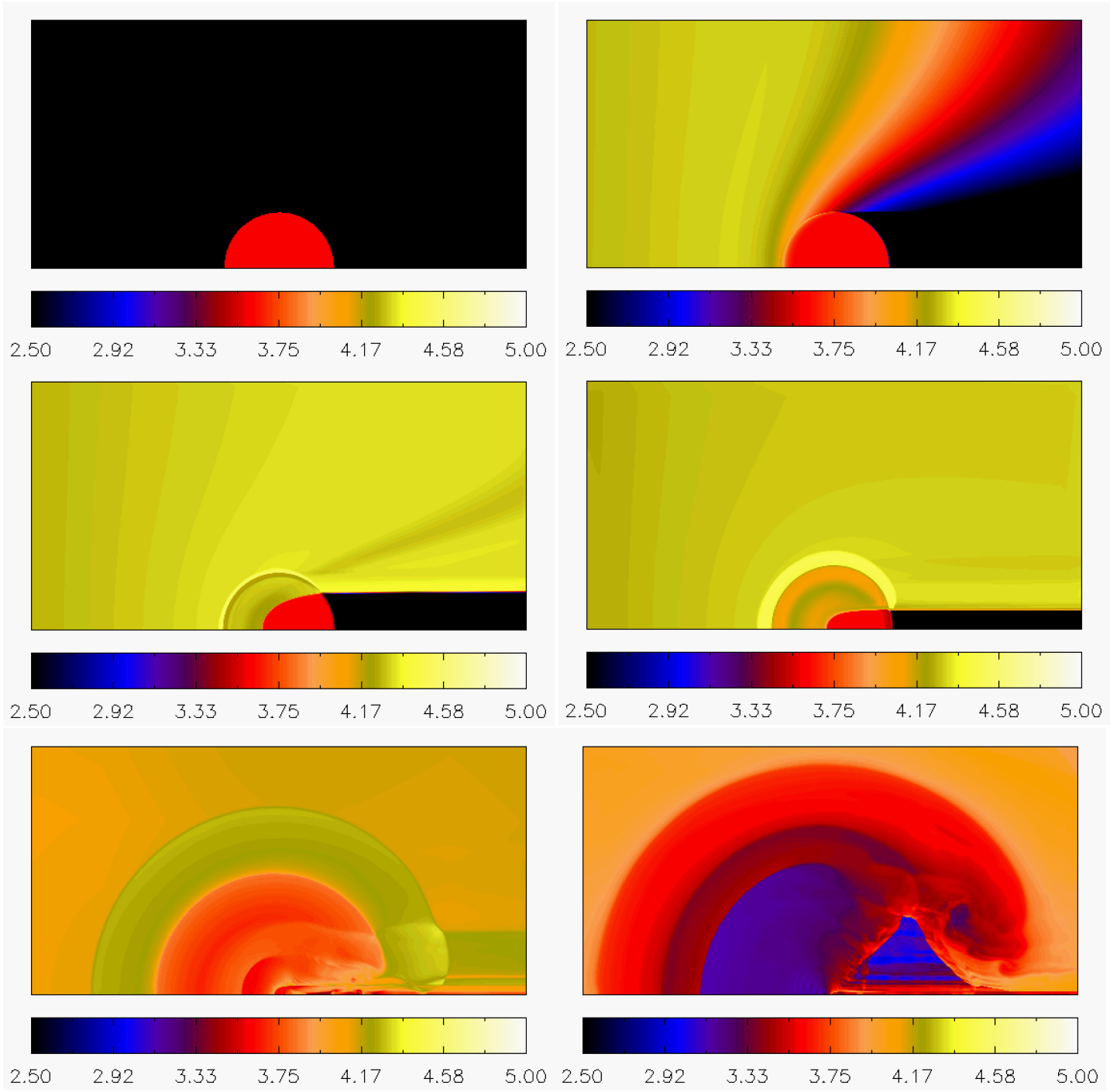

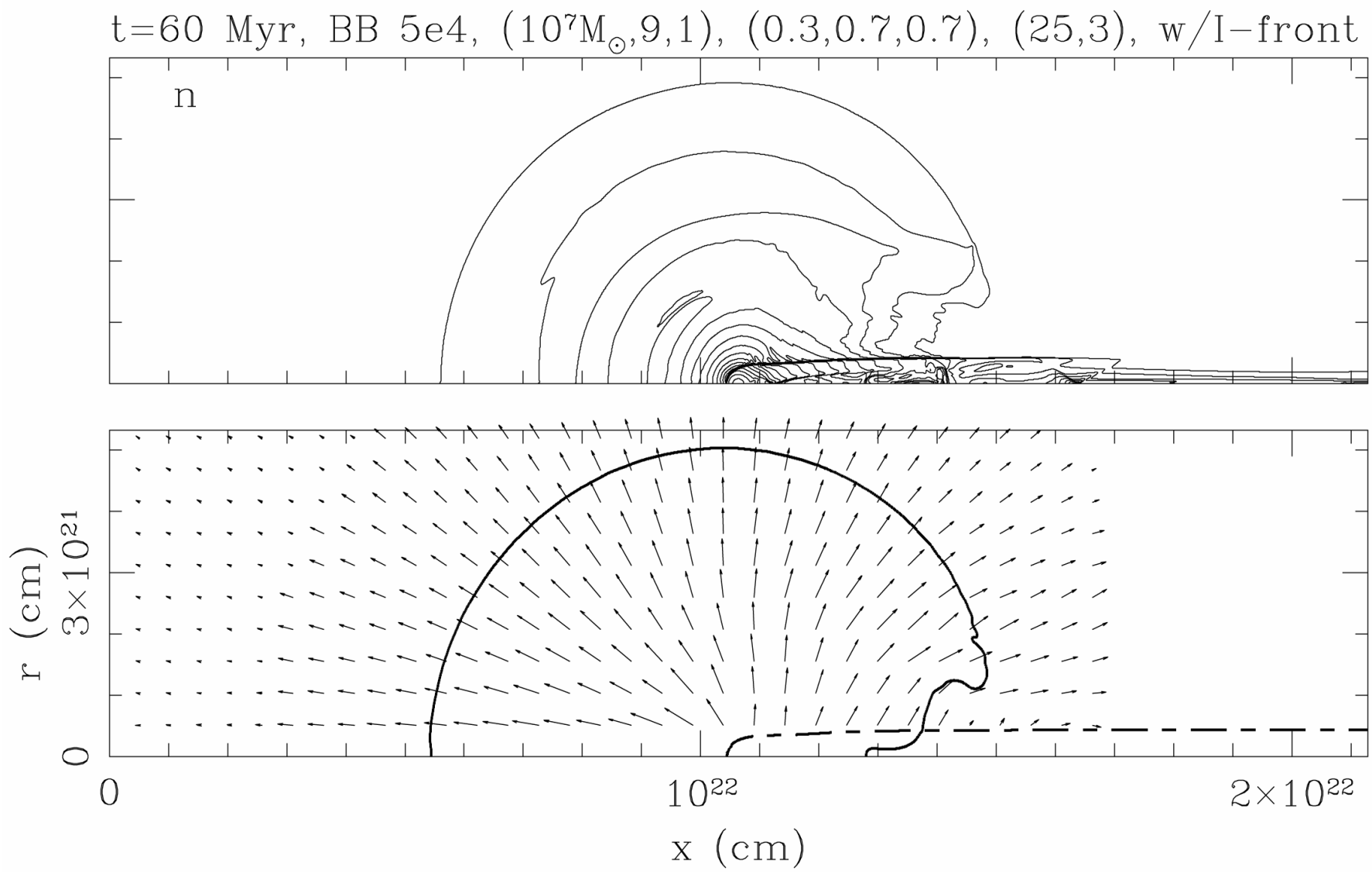
t=60 Myr, BB 5e4, (10⁷M⊙,9,1), (0.3,0.7,0.7), (25,3), w/I−front
n
r (cm)
3×10²¹
0
0
10²²
2×10²²
x (cm)

1 = IGM shock.

2 = contact discontinuity which separates shocked halo wind (between 2 and 3) from swept-up IGM (between 1 and 2).

3 = wind shock.

between 3 and 4 = supersonic wind.

4 = I-front.

5 = boundary of gas initially inside minihalo at z = 9.

6 = shock in shadow region caused by compression of shadow gas by shock-heated gas outside shadow.

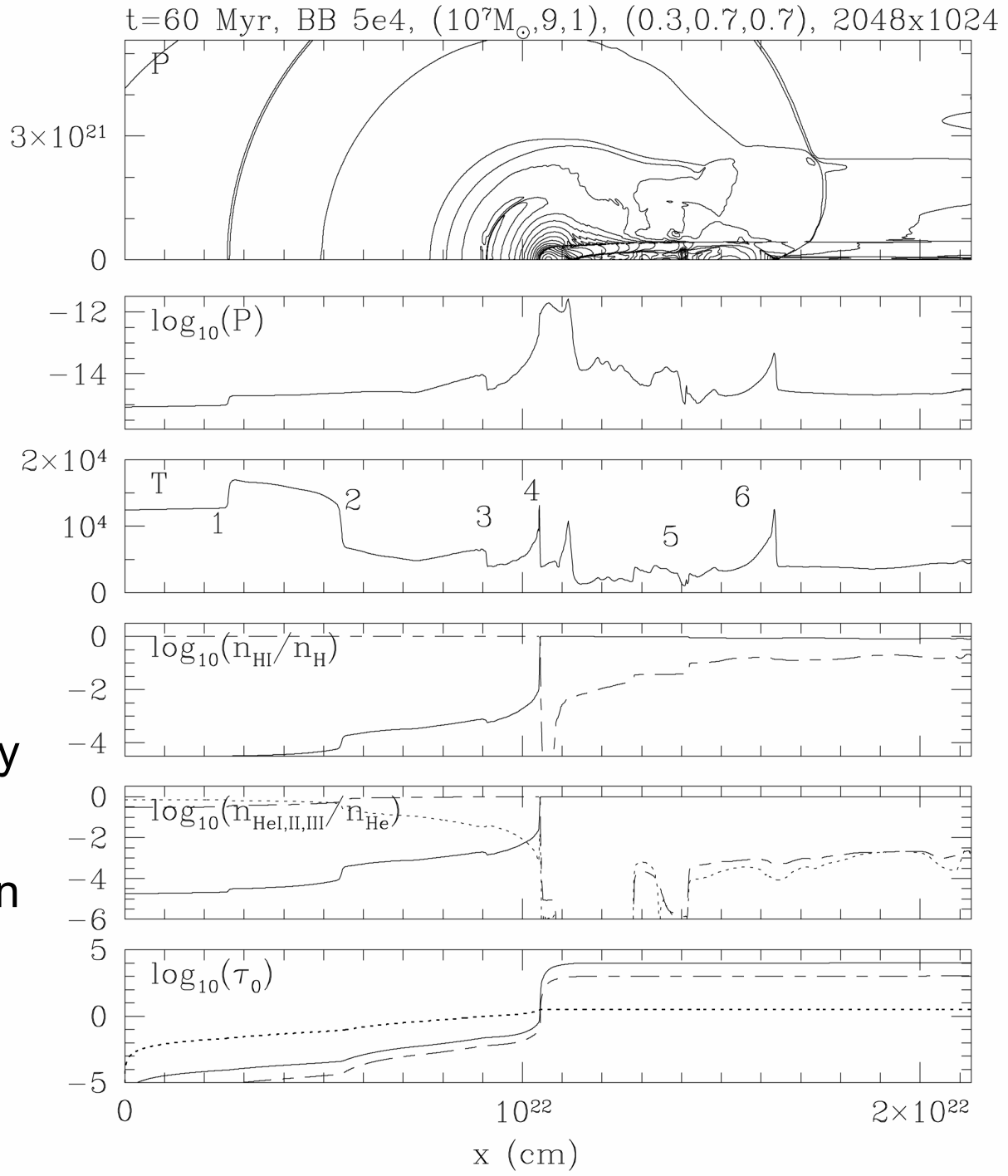

ANIMATIONS

Pop II

- **TEMPERATURE**
- **DENSITY**
- **H I**
- **He II**
- **C IV**

Pop III

- **TEMPERATURE**
- **DENSITY**
- **H I**
- **He II**
- **C IV**

Ionizing Photons Consumed Per Minihalo Atom

- $\xi(t)$ = # photons consumed per minihalo atom over time t.
- $(M_{halo}, z_{initial}, F_0) = (10^7 M_{sun}, 9, 1)$.

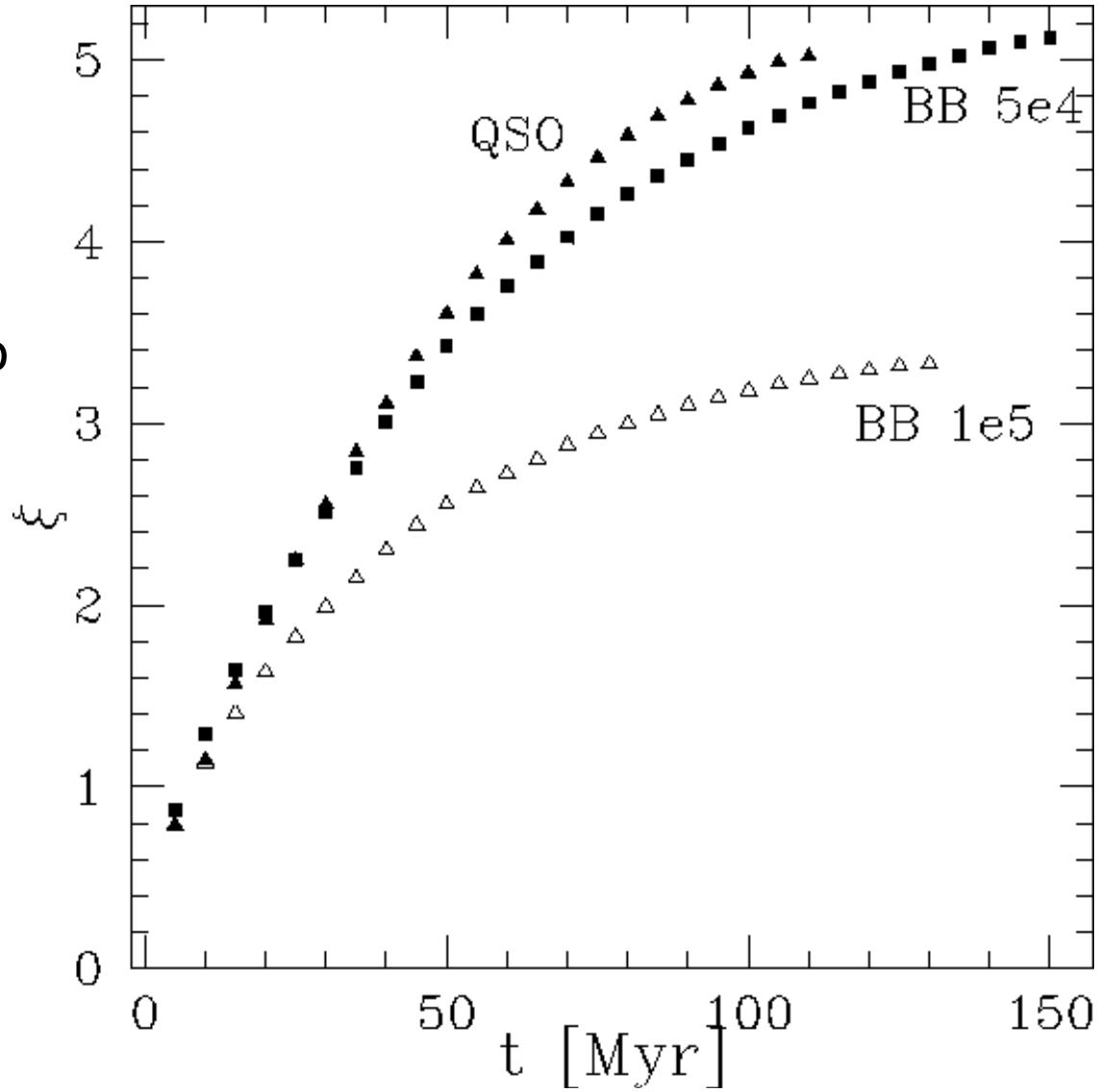

Iliev, Shapiro, and Raga (2004)

Evaporation times

Ionizing photon consumption

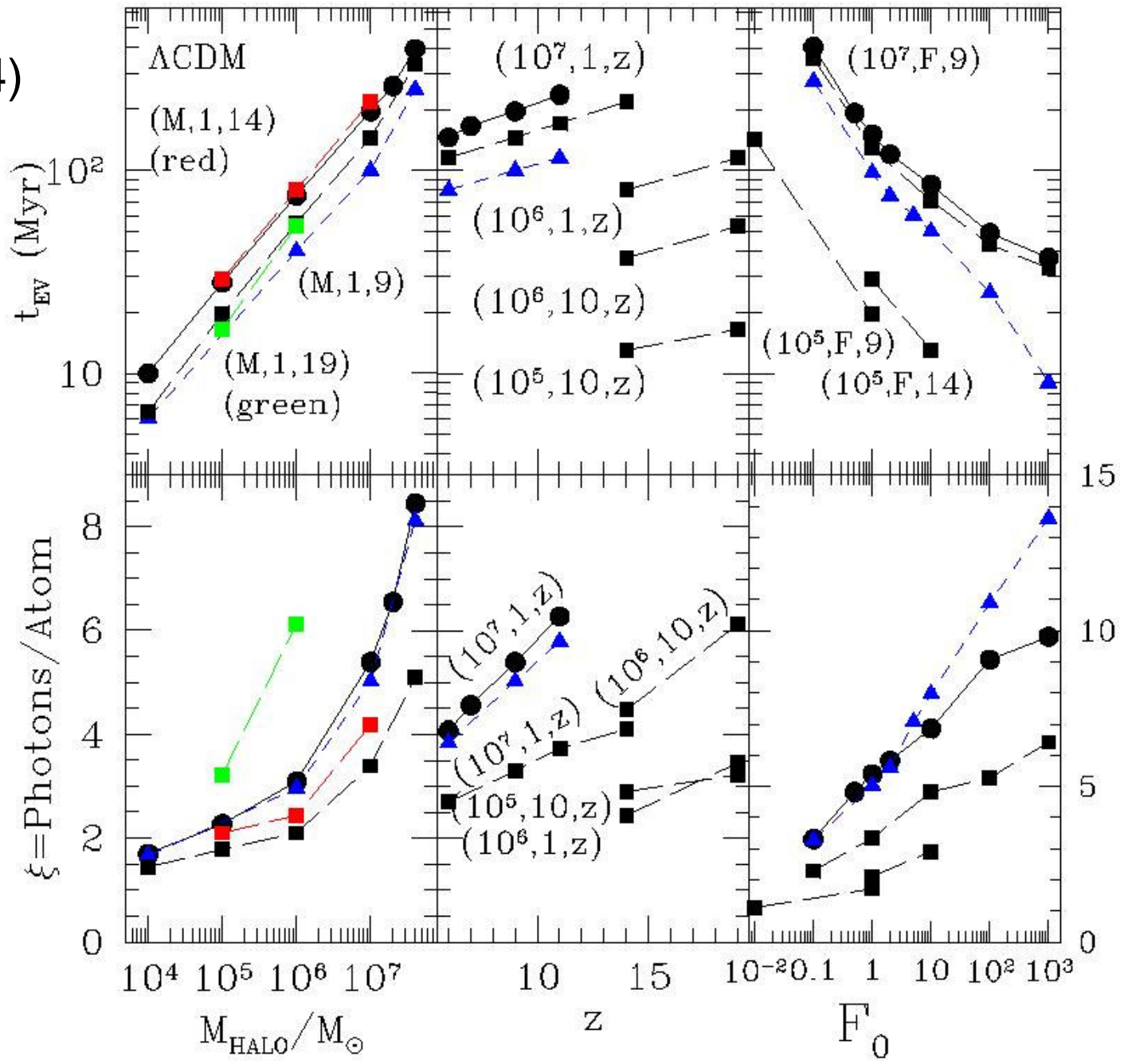

Part II:

The Effect of Small-Scale Structure on Reionization

Effect of Minihalo Photon Consumption on Reionization (Iliev, Scannapieco & Shapiro, 2004)

- Let each source halo create its own expanding spherical I-front.
- I-front speed is slowed by minihalo trapping and evaporation.
- Integrate over statistical distribution of source halo masses and turn-on epochs until neighboring H II regions overlap => reionization finished.
- Minihalos increase photon consumption by factor of ~2, delaying reionization.

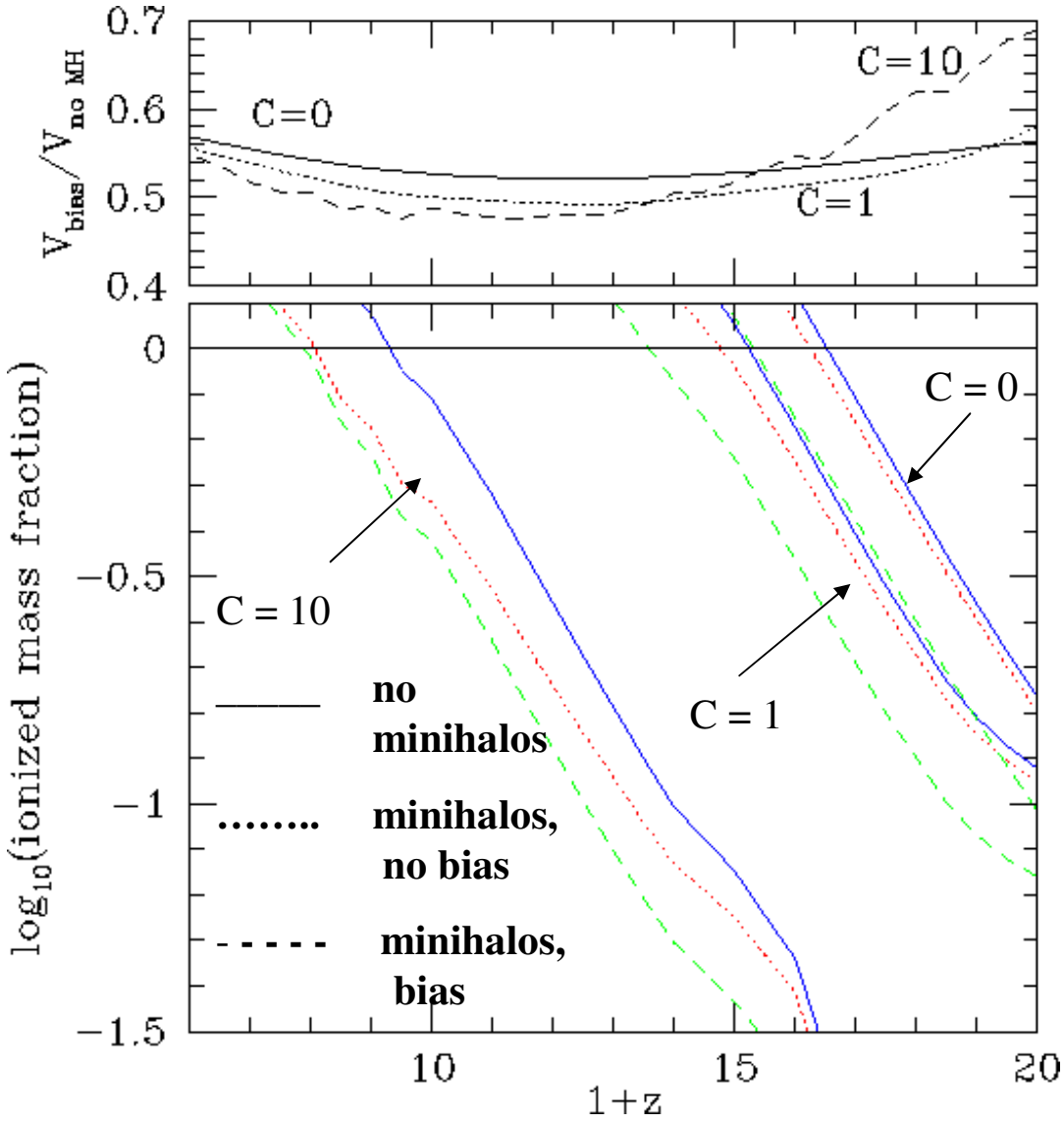

Effect of Minihalo Photon Consumption on Reionization (Iliev, Scannapieco & Shapiro, 2004)

- Delaying reionization slows the rise of electron scattering depth thru IGM.
- Enough delay to satisfy the GP constraint by ending reionization at z~6 => too little τ_{es} to explain WMAP polarization.
- To satisfy both GP and WMAP: Prolonged reionization required => either ionizing radiation release efficiency must drop or gas clumping outside minihalos must rise over time or both.

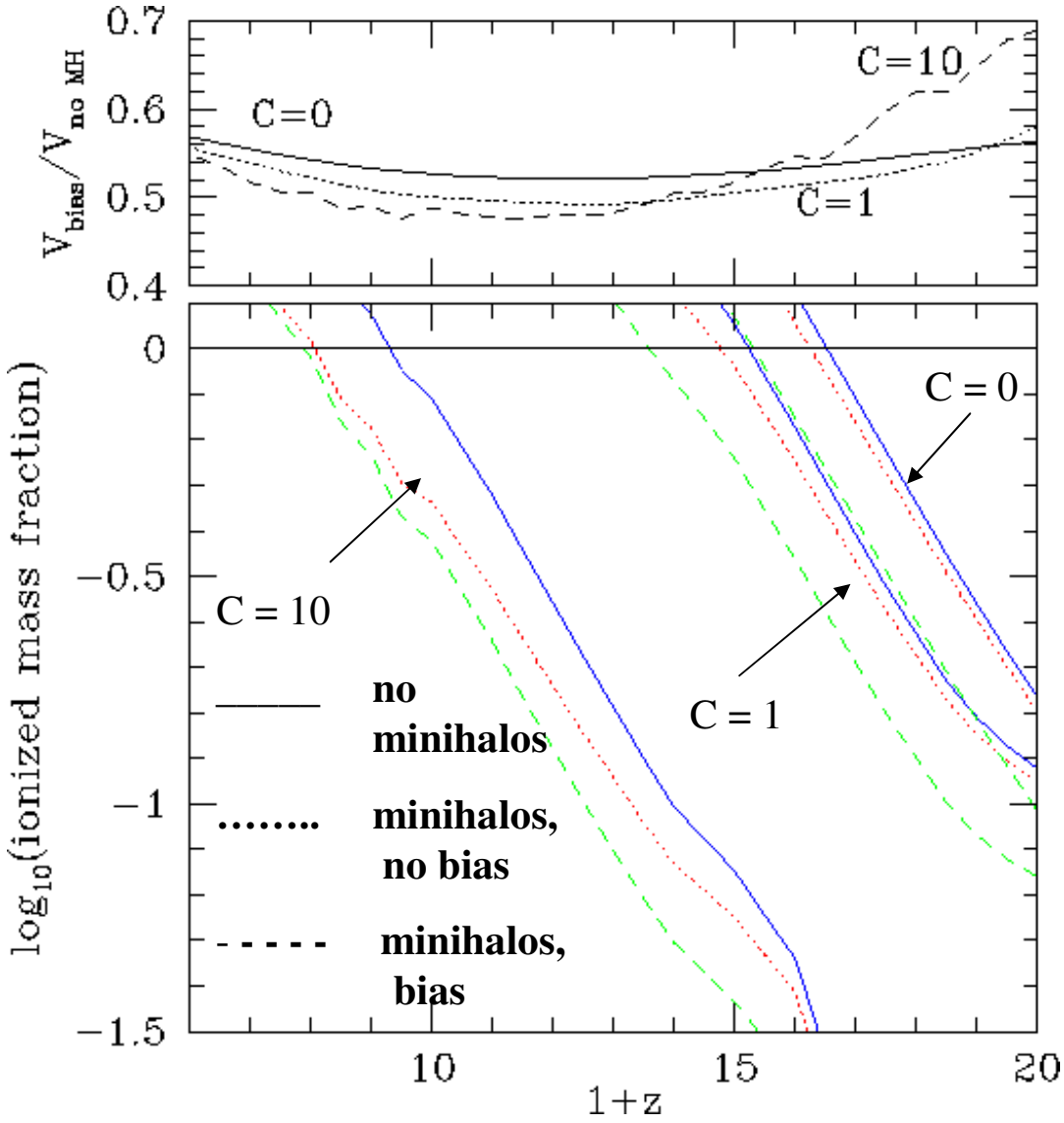

Effect of Minihalo Photon Consumption on Reionization with IGM Clumping C(z)

- We use N-body simulations to calculate the IGM clumping factor for gas **outside** halos.
- C(z) increases with time

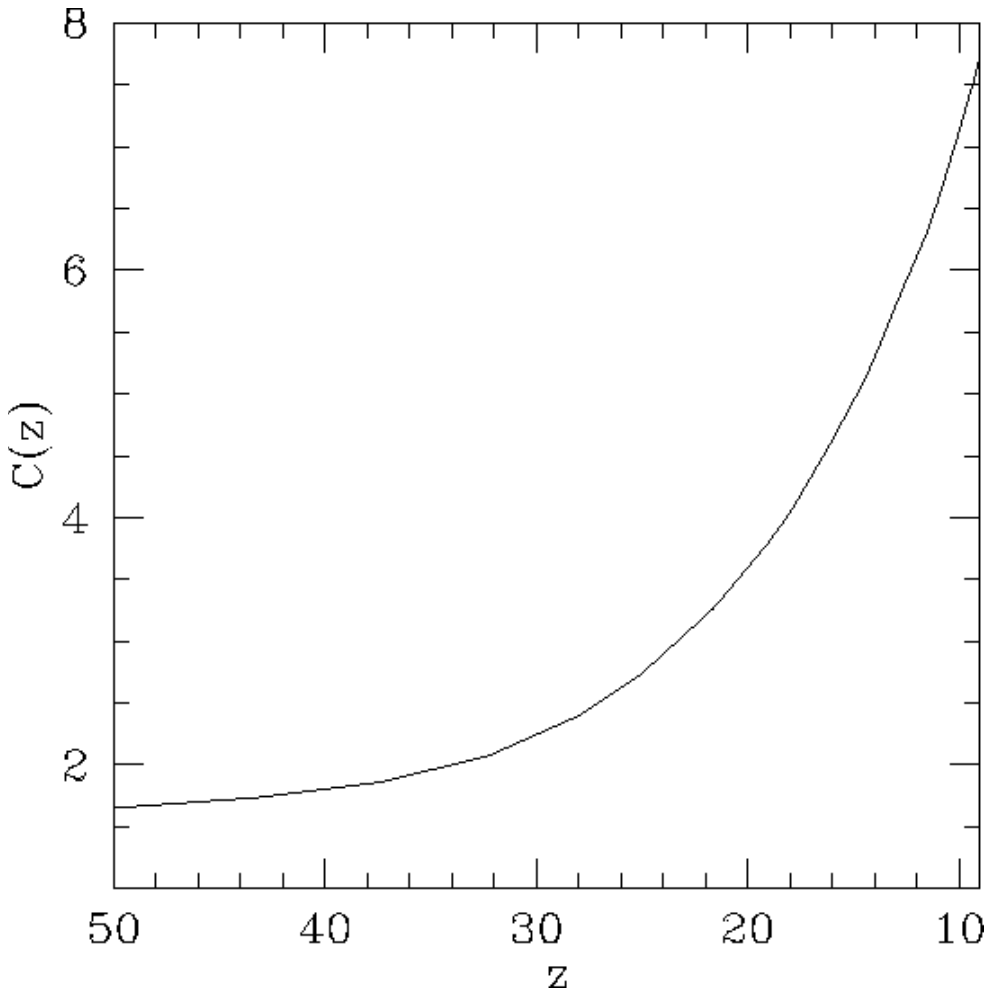

Effect of Minihalo Photon Consumption on Reionization with IGM Clumping C(z)

- C(z) increases with time → helps to prolong reionization epoch
- Minihalos still increase photon consumption by factor of ~2, delaying reionization ($\delta z \sim 2$).
- e.g. If z_{ov}=9.5 requires 14 ionizing photons/atom, then minihalos make z_{ov}=7.5 with 33 photons/atom.
- Does C(z) prolong reionization enough to satisfy both WMAP and GP?

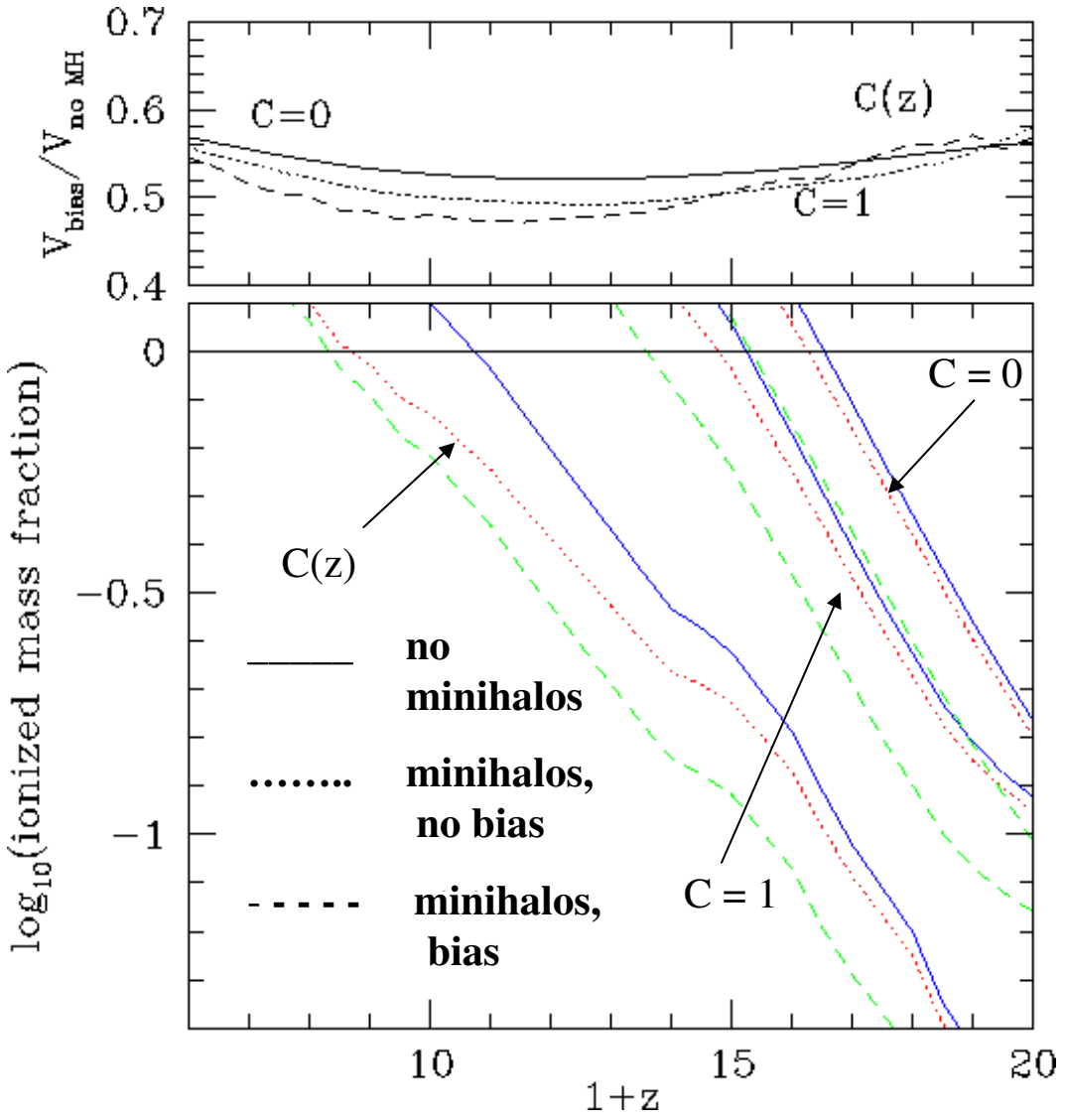

Effect of Minihalos and Time-Varying Clumping of IGM on Reionization

- Delaying reionization slows the rise of electron scattering depth thru IGM.
- Enough delay to satisfy the GP constraint by ending reionization at z~6 => still too little τ_{es} to explain WMAP polarization.
- C(z) helps, but to satisfy both GP and WMAP, probably also need ionizing radiation release efficiency to drop over time as well.

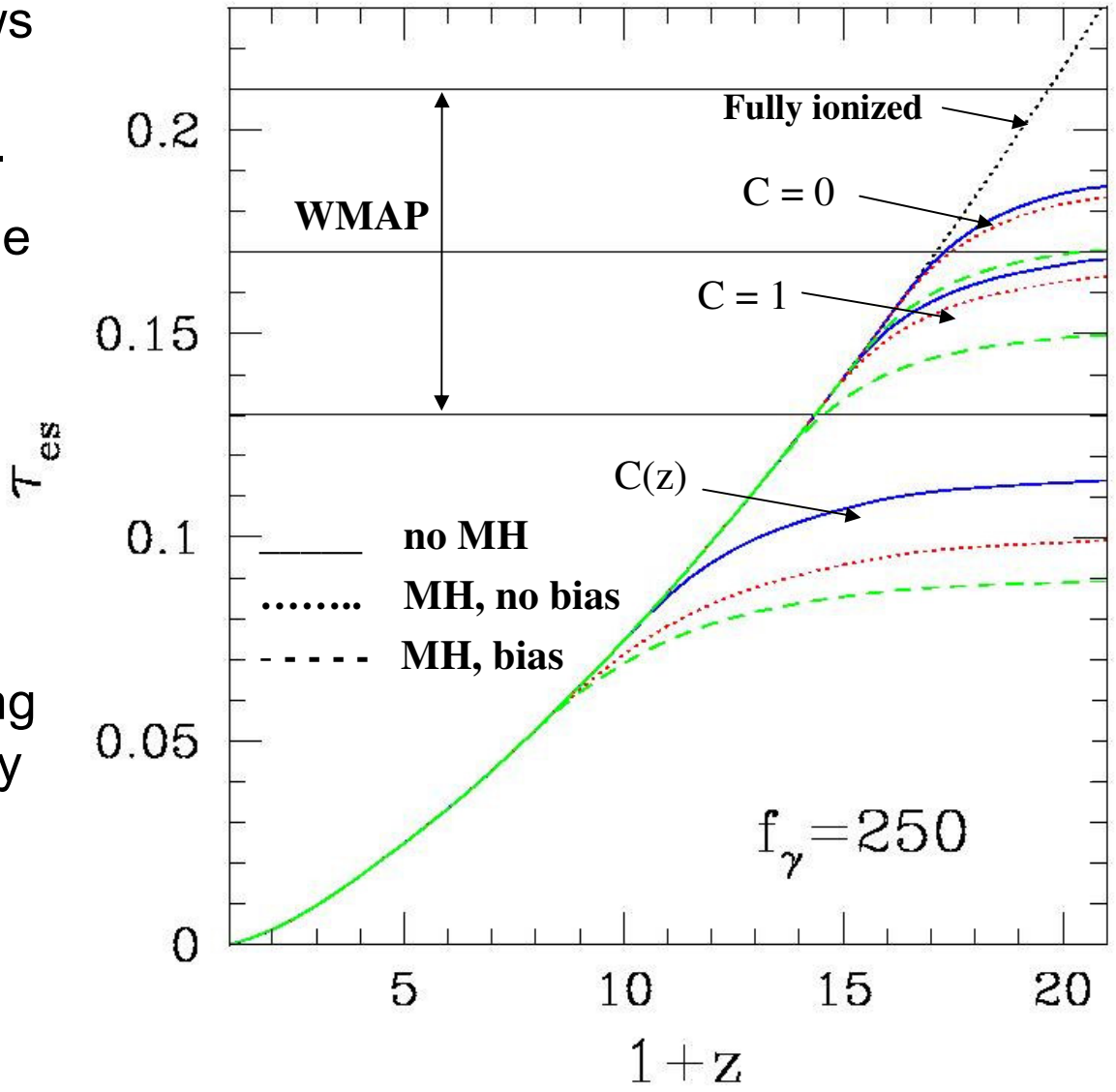

21-cm From Minihalos and the IGM Before Lyman-α Pumping

Paul R. Shapiro

University of Texas at Austin

KITP, UC Santa Barbara,

September 16, 2004

Part I:

On the Detectability of the Cosmic Dark Ages: 21-cm Lines from Minihalos

Collisional decoupling of the spin temperature T_S from T_{CMB} for different overdensities with respect to mean IGM.

bottom to top : δ =0, 5, 10, 20, 50, 100 and 200 at z=9 (left panel) and z=19 (right panel).

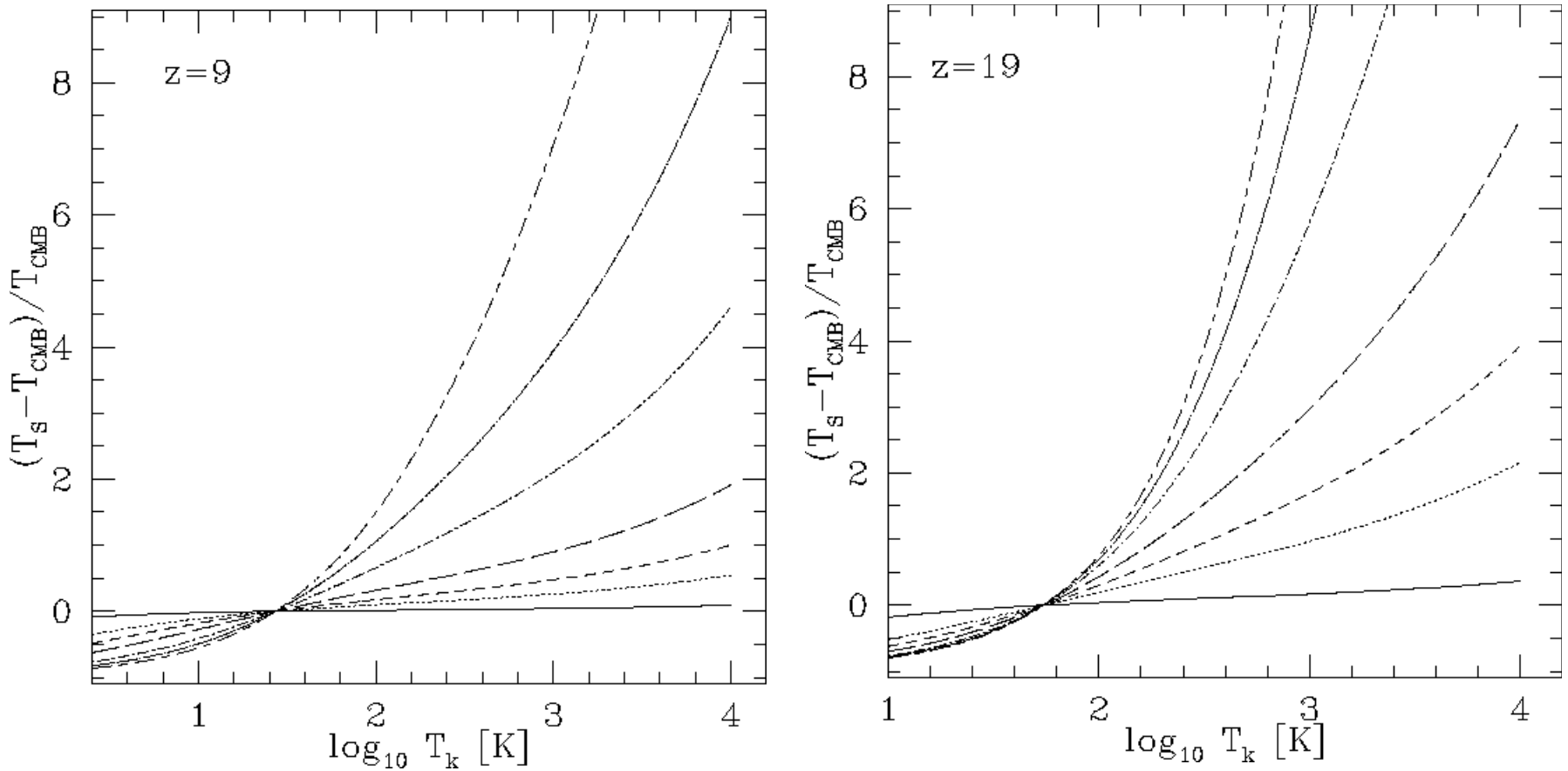

Iliev, Shapiro, Ferrara, Martel (2002)

Minihalo radiation background. Average observed differential antenna temperature δT_b and average differential flux per unit frequency δF_ν for beam size of $\Delta\theta_{beam} = 10'$ at the redshifted 21 cm line frequency due to minihalos vs. redshift z for ΛCDM models with power spectrum tilts n_p = 0.9, 1.0, and 1.1, as labeled.

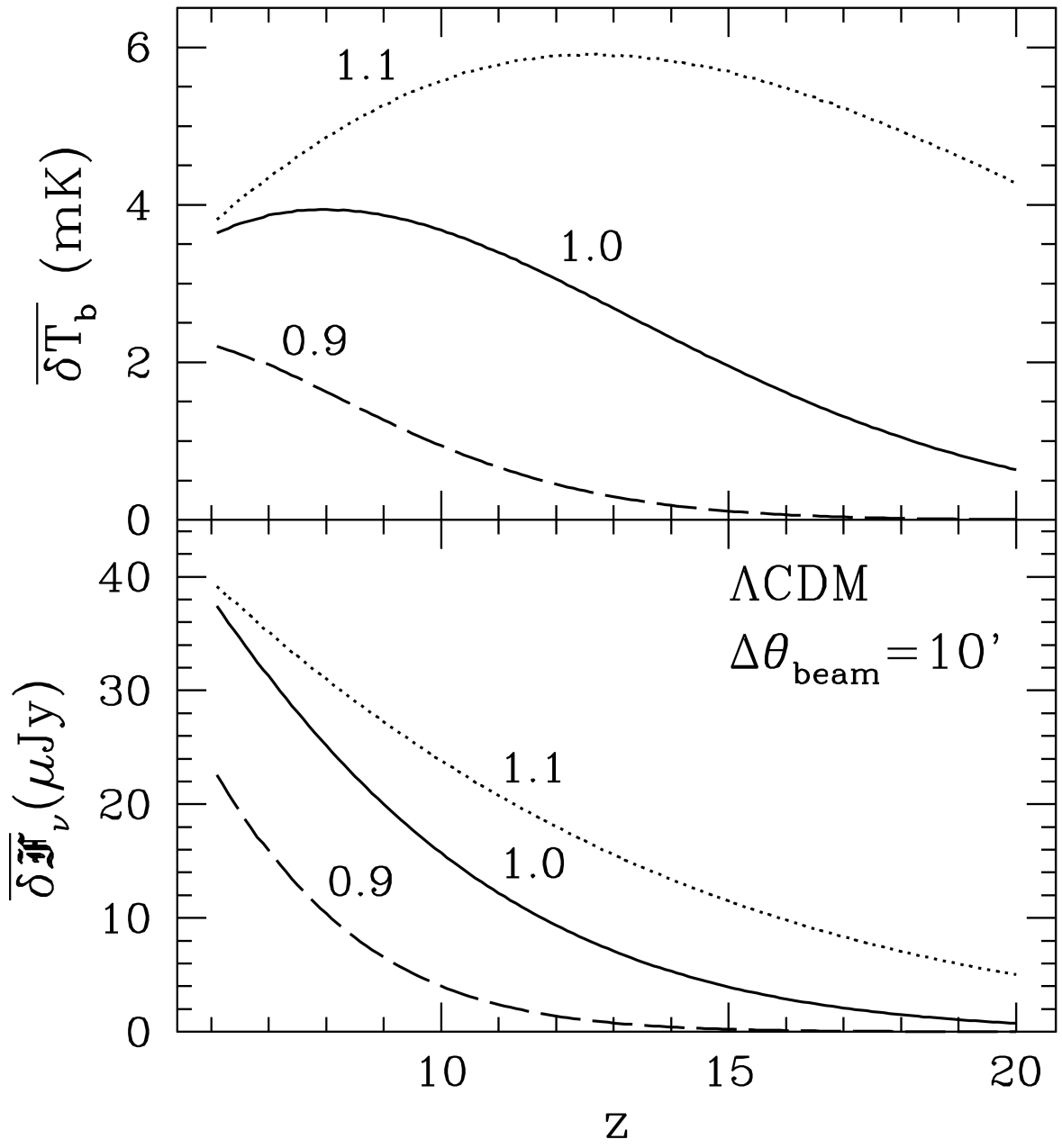

ANGULAR FLUCTUATIONS IN THE 21-CM EMISSION BACKGROUND. The clustering of minihalos as structure grows hierarchically in a CDM universe causes angular fluctuations in the 21-cm radiation background. To illustrate this, we have performed N-body simulations of halo formation in ΛCDM. Radio maps of the 21-cm emission from the simulation cubes at z = 9 are shown.

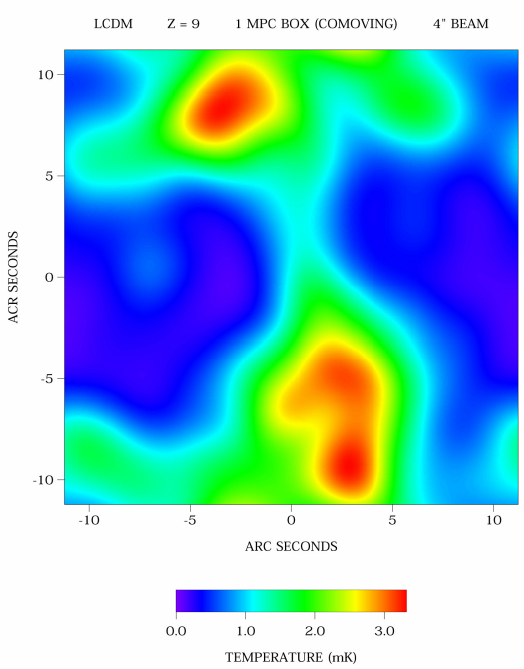

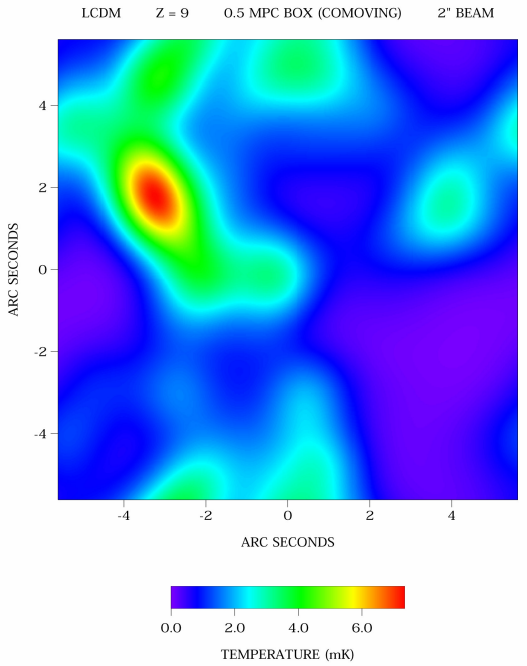

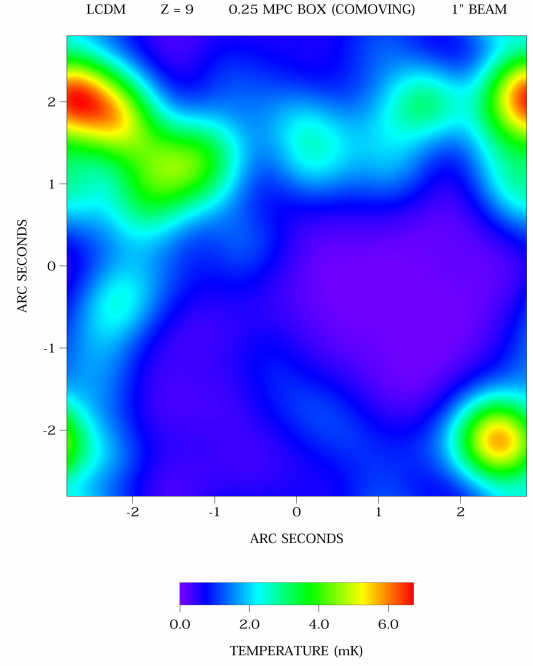

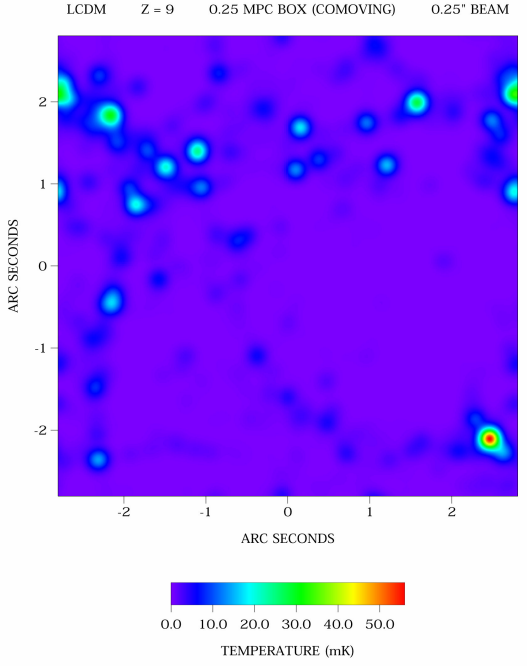

Predicted 3-σ differential antenna temperature fluctuations for different beam sizes.

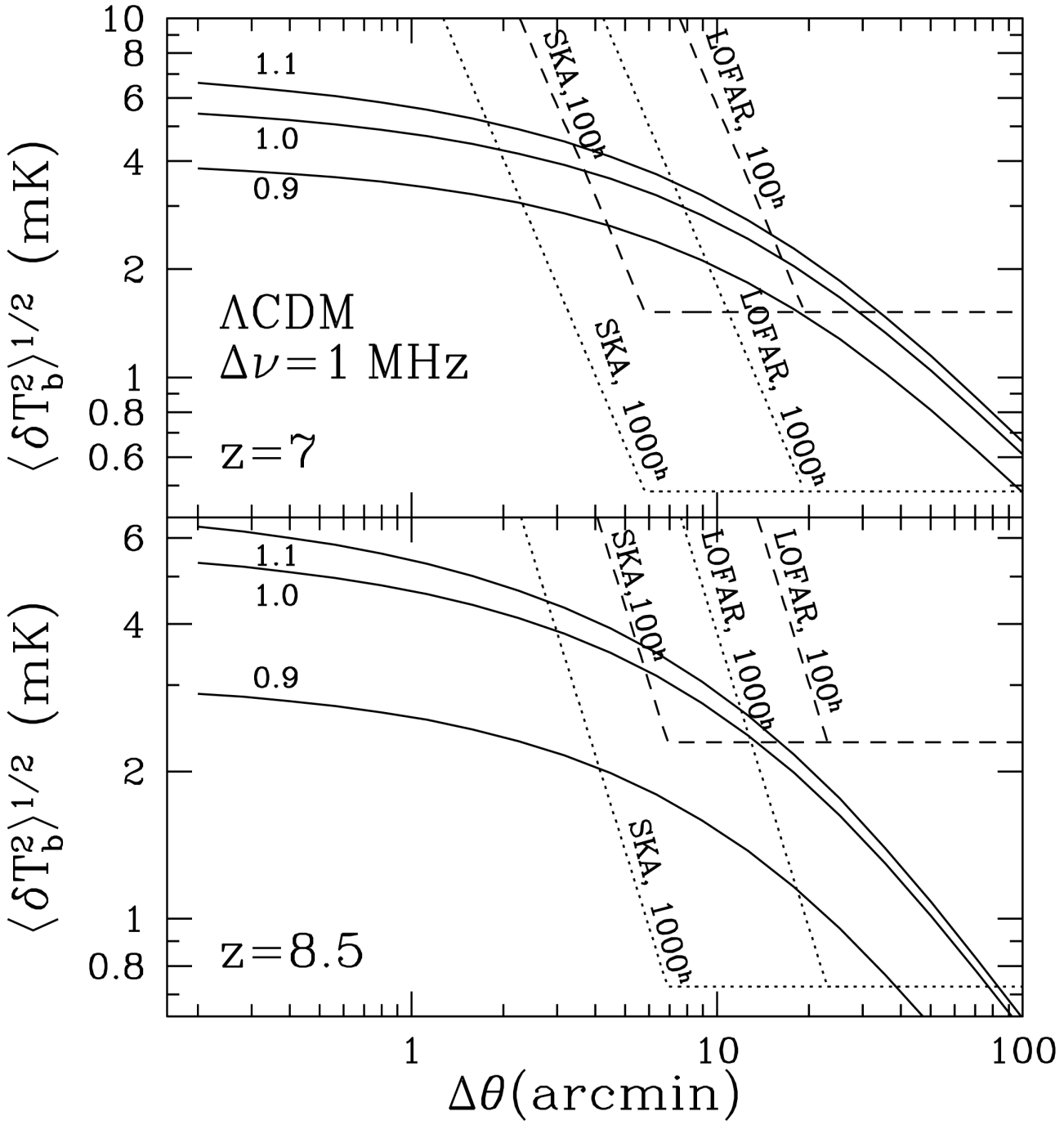

Predicted 3-σ differential antenna temperature fluctuations for different redshifts.

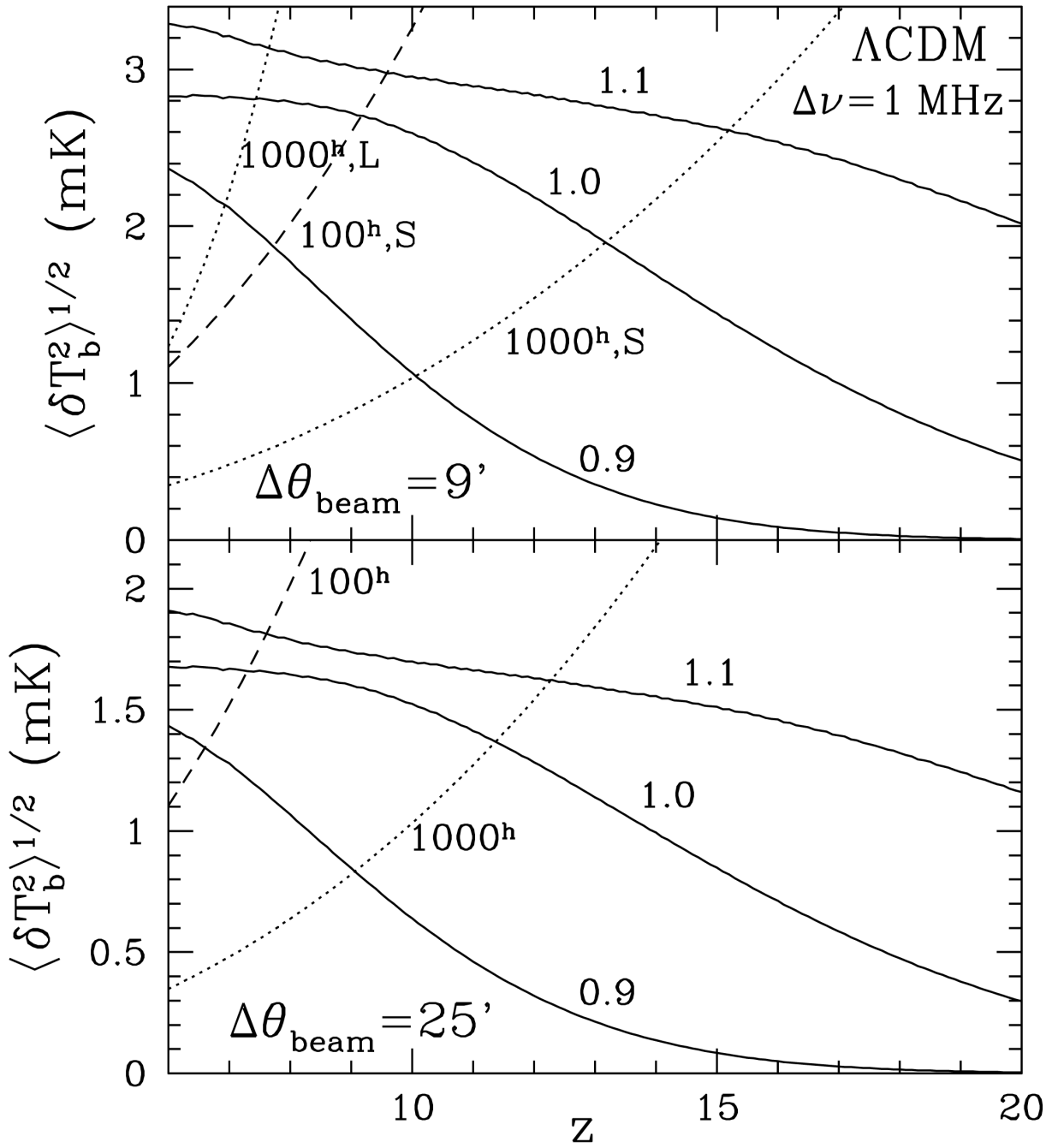

Detectability of Angular Fluctuations

- These 3-σ fluctuations should be observable with both LOFAR (300m filled aperture) and SKA (1km filled aperture) with integration times of between 100 and 1000 hours.
- For a 25' beam, for example, 3-σ fluctuations can be detected for untilted ΛCDM by both with a 100h integration for z ~ 6 – 7.5 and a 1000h integration for z <~ 11.5, while for a 9' beam, SKA can detect them after 100h for z <~ 9 and after 1000h for z <~ 13.

Martel, Shapiro, Iliev, Scannapieco, Ferrara (2003)

21-cm absorption line profiles for individual minihalos of different mass at z = 9. Transmission factor versus received frequency ν_{rec} at z = 0, for line of sight through minihalo center (i.e. zero impact parameter).

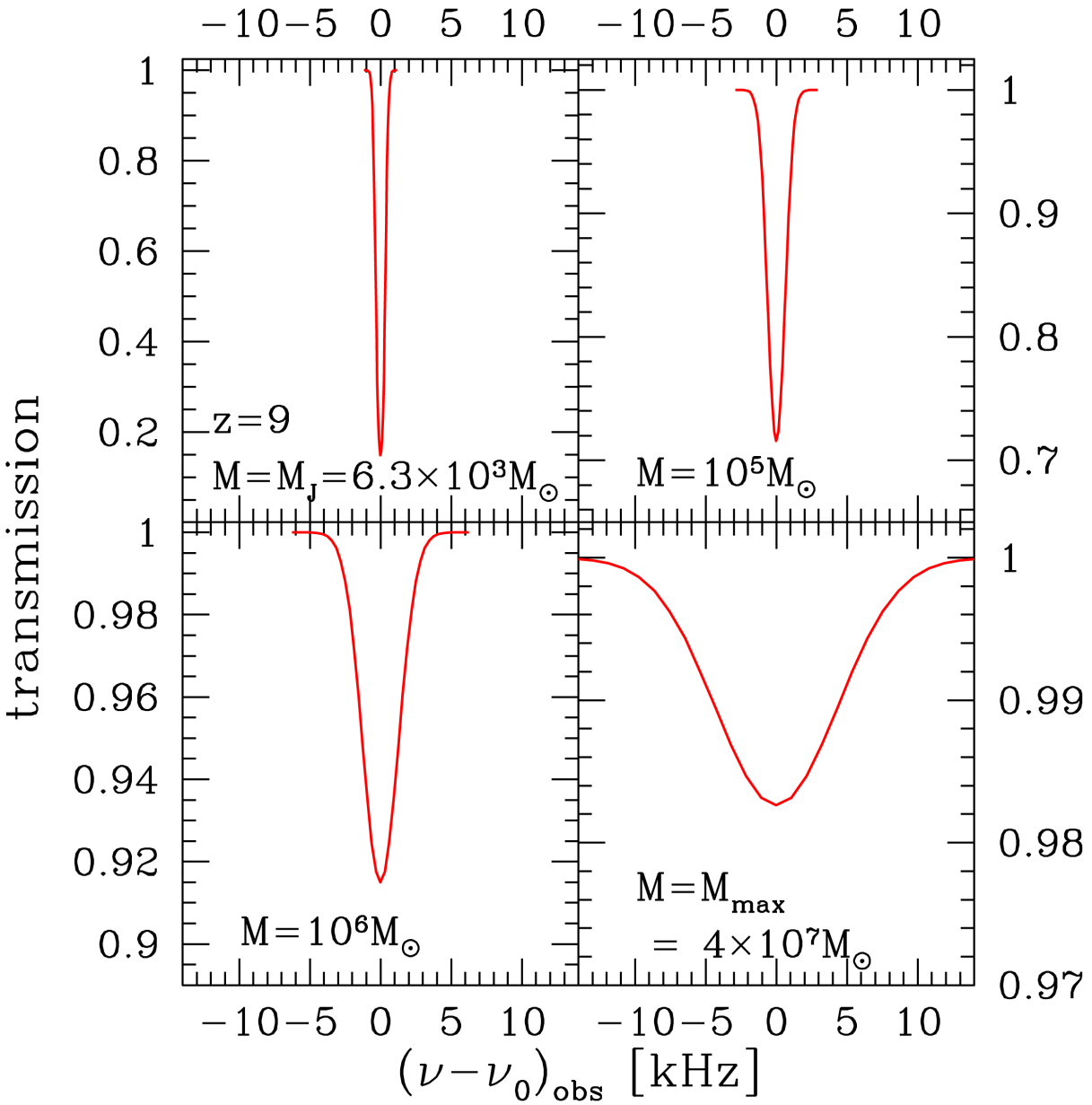

21-cm Emission from Minihalos vs. Shock-heated Gas outside Virialized Regions

(Shapiro, Ahn, Alvarez, Martel, Iliev, Ryu 2004)

- Shock-heated IGM outside of the minihalos may also contribute to the 21-cm background, despite its less effective collisional pumping (Furlanetto and Loeb 2003).
- To quantify this, we simulated the gas and N-body dynamics of cosmic structure formation in LCDM before reionization, to compute the spin temperature at each point and map the differential brightness temperature vs. redshift.
- TVD/PM simulations of 0.7 Mpc comoving box size used 512^3 cells and 256^3 particles.

TOTAL Z=8

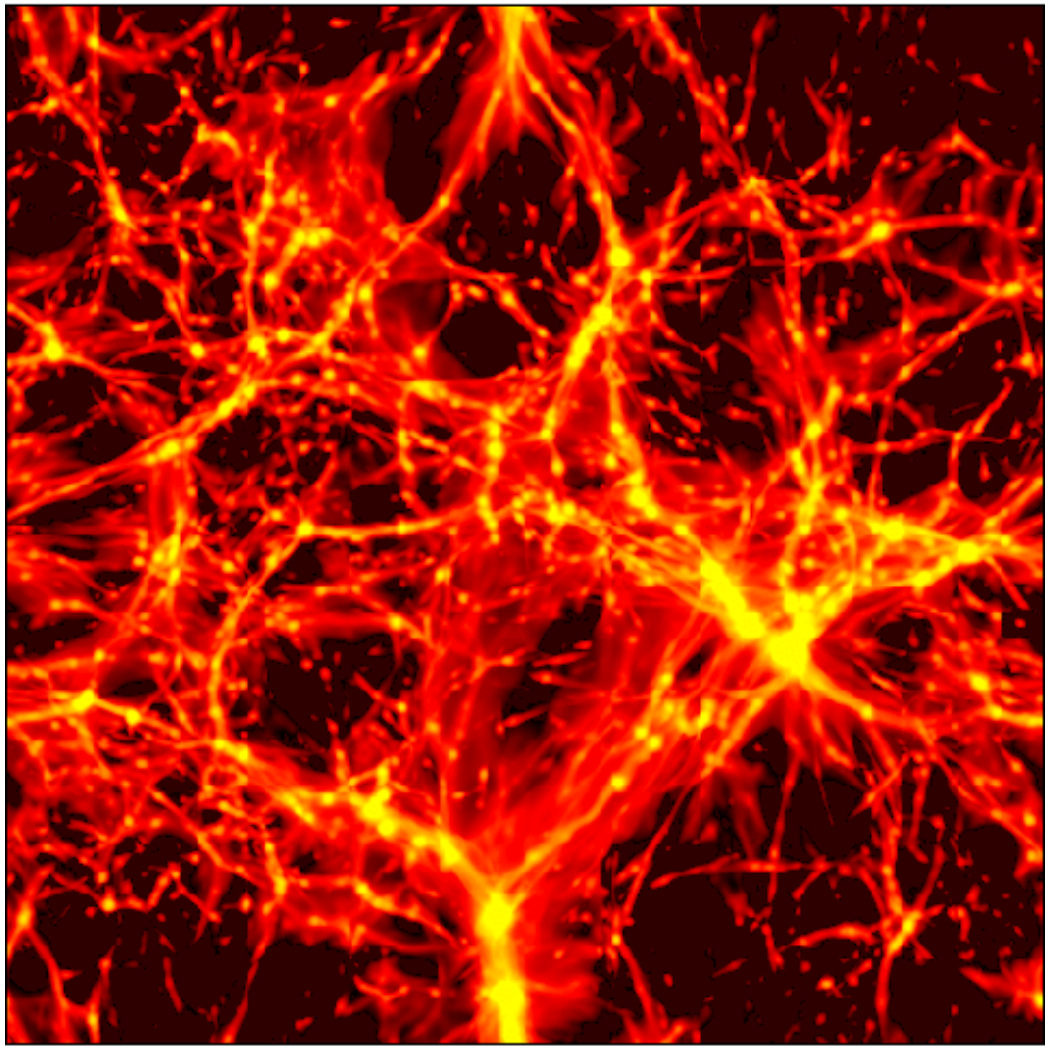

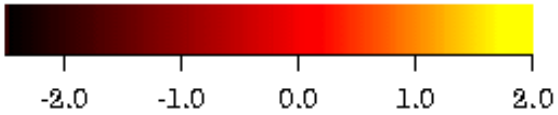

LOG 10 [DIFFERENTIAL BRIGHTNESS TEMPERATURE] (mK)

WITHOUT HALOS Z=8

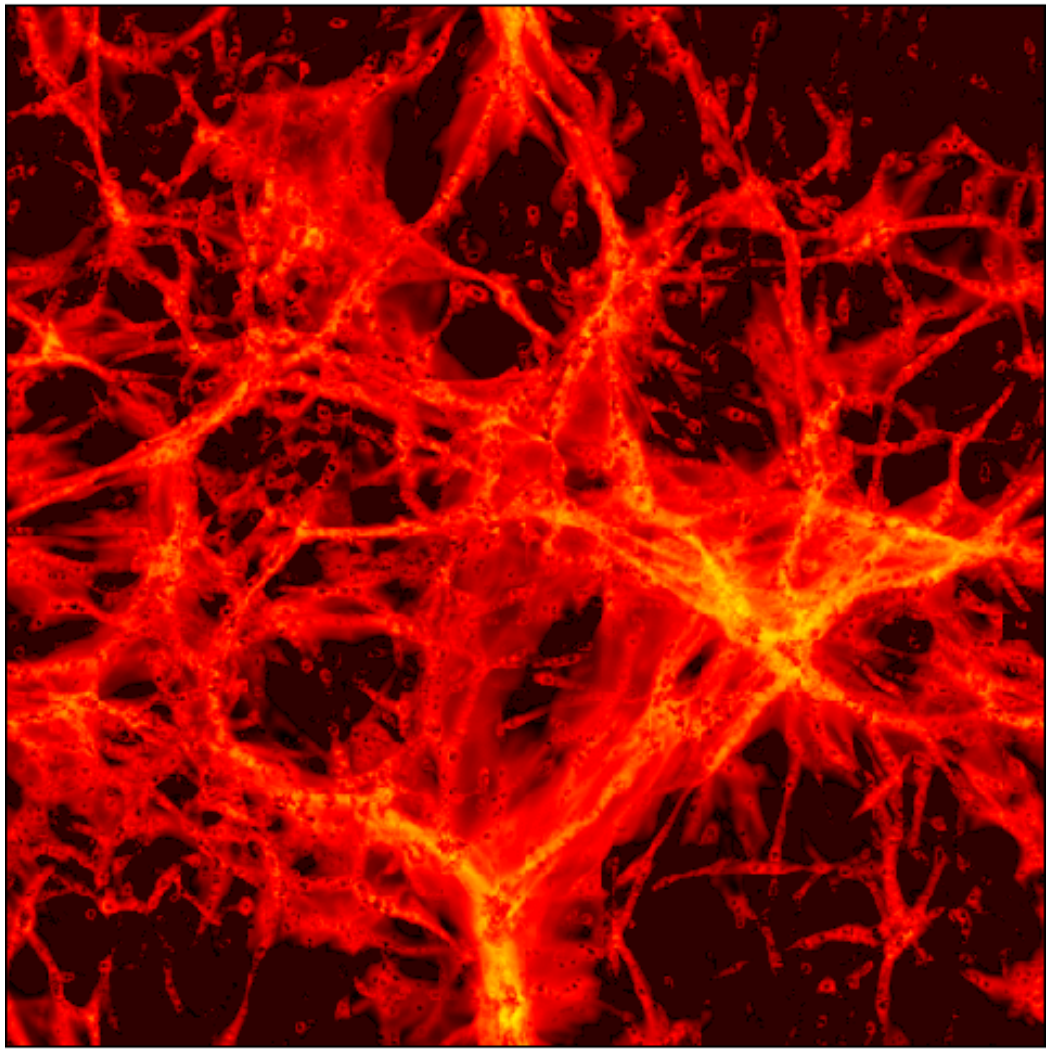

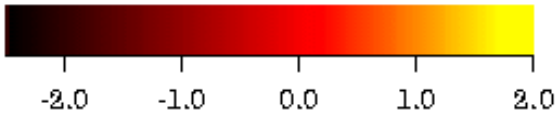

LOG 10 [DIFFERENTIAL BRIGHTNESS TEMPERATURE] (mK)

MINIHALOS ONLY Z=8

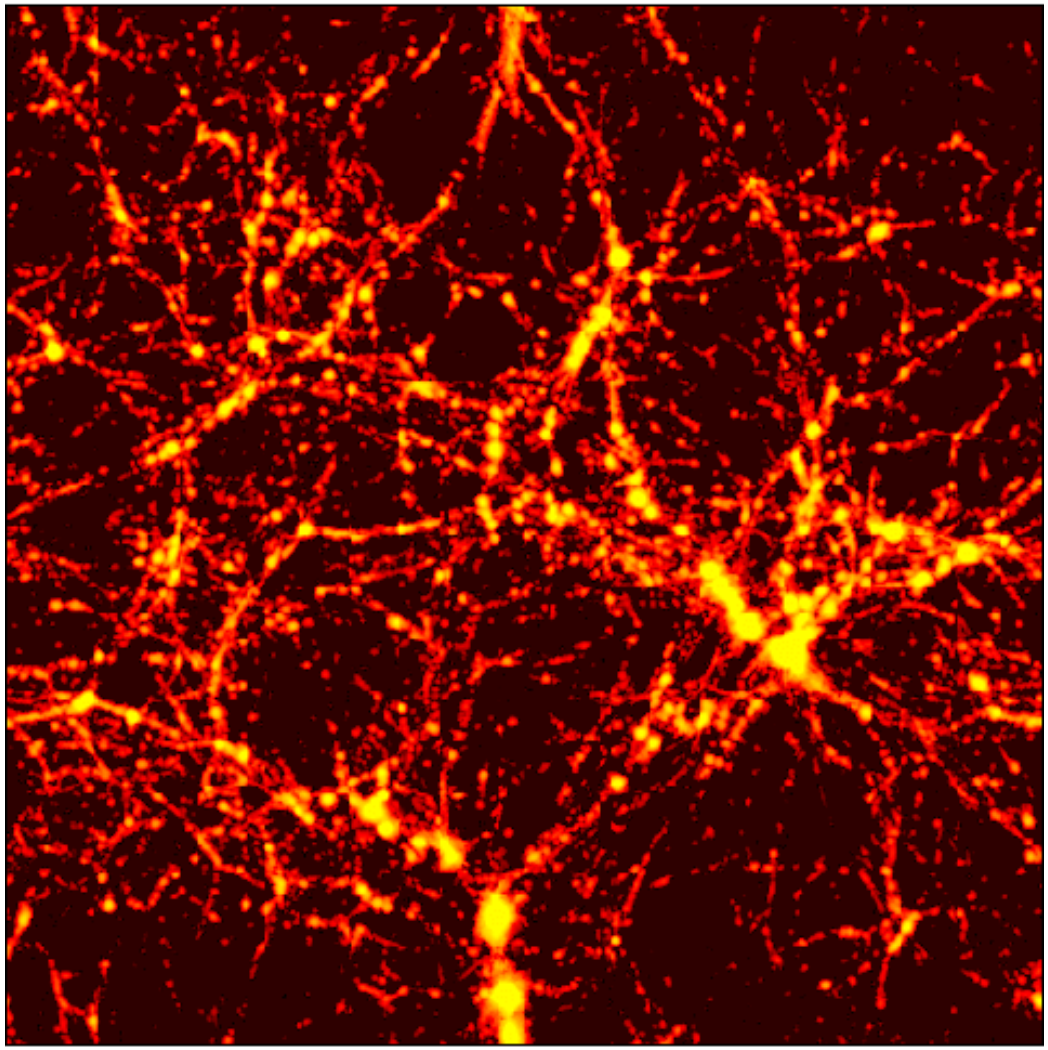

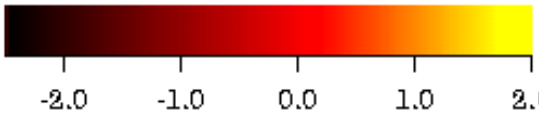

LOG 10 [DIFFERENTIAL BRIGHTNESS TEMPERATURE] (mK)

Minihalos vs. IGM

- Mean brightness temperature dominated by minihalos for z < 20.
- For z > 16, IGM contribution changes from emission to absorption.
- At z > 20, IGM absorption dominates over minihalo emission.
- At z > 20, mean brightness temperature same as uniform IGM

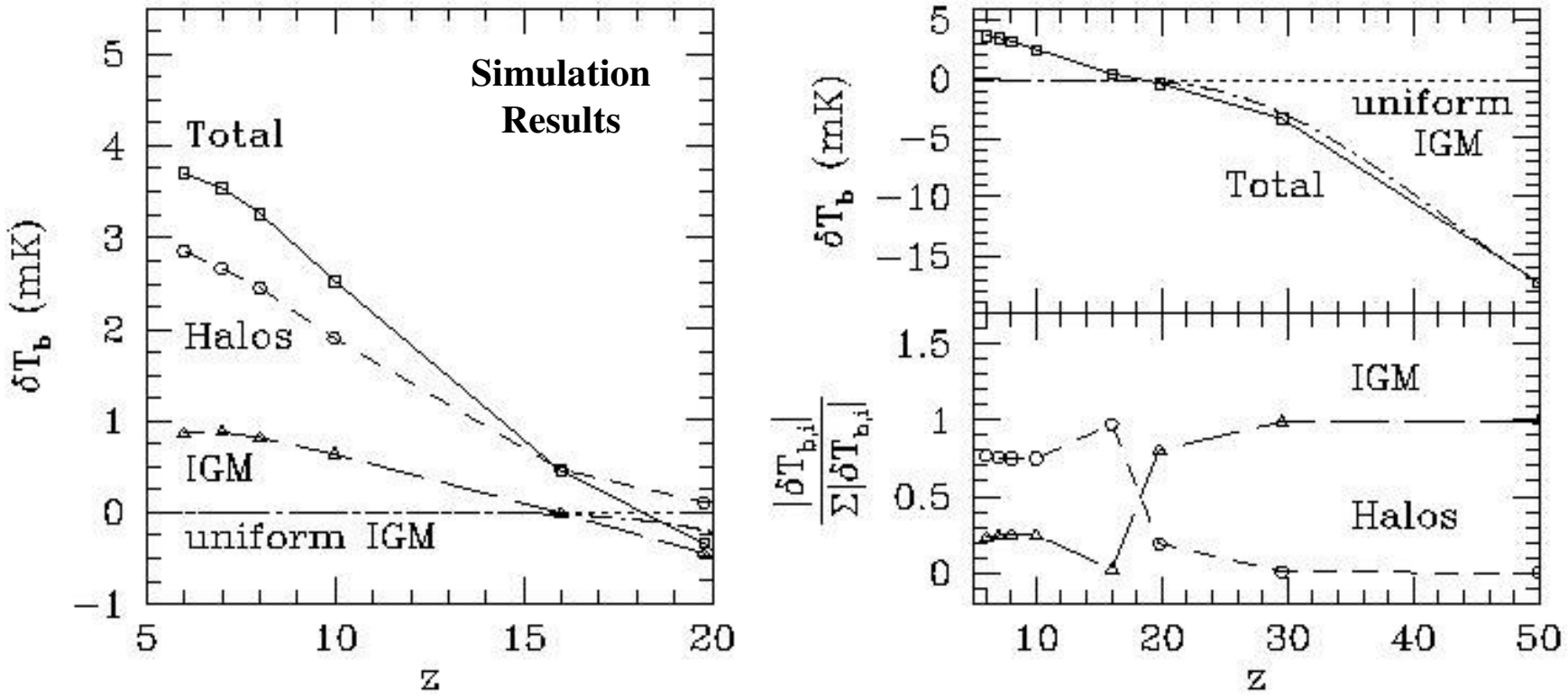

Minihalos vs. IGM

- Mean brightness temperature dominated by minihalos for z < 20.
- For z > 16, IGM contribution changes from emission to absorption.
- At z > 20, IGM absorption dominates over minihalo emission.
- At z > 20, mean brightness temperature same as uniform IGM

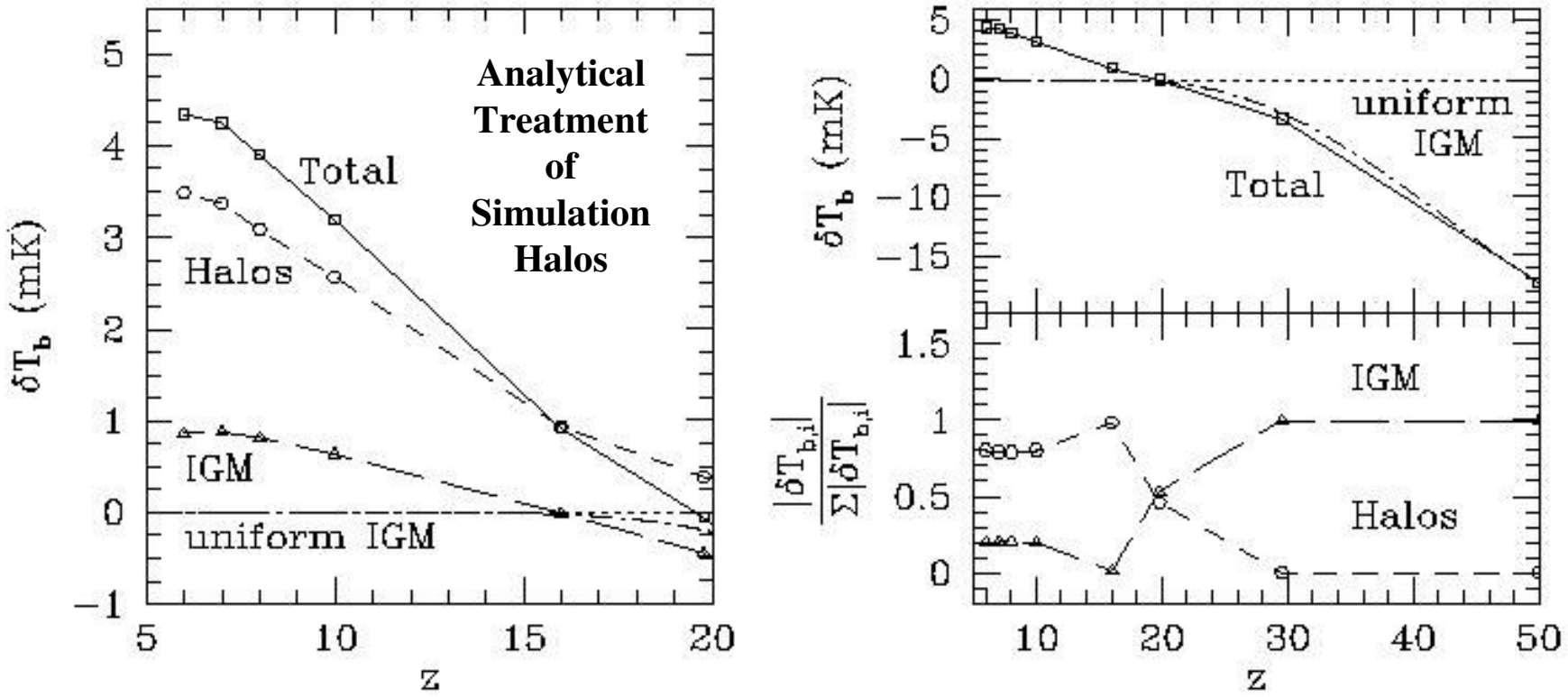

Minihalos vs. IGM

- Mean brightness temperature dominated by minihalos for z < 20.
- For z > 16, IGM contribution changes from emission to absorption.
- At z > 20, IGM absorption dominates over minihalo emission.
- At z > 20, mean brightness temperature same as uniform IGM

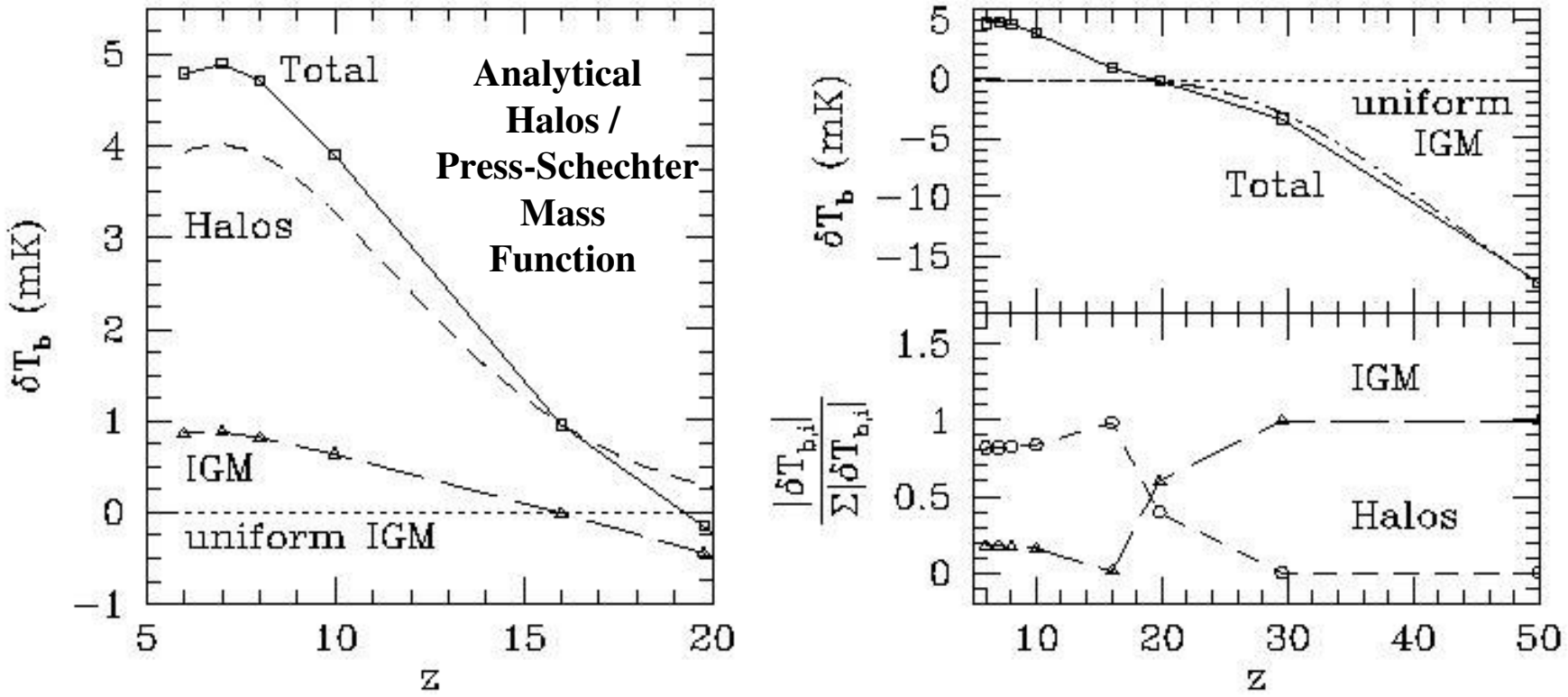

Galaxy Formation and the Intergalactic Medium Research Group

Members:

- Paul Shapiro
- Hugo Martel
- Kyungjin Ahn
- Marcelo Alvarez

External Collaborators:

- Alejandro Raga (Mexico)
- Ilian Iliev (CITA), Andrea Ferrara (Italy), & Evan Scannapieco (KITP/UCSB)
- Hyesung Kang & Dongsu Ryu (Korea)

Computer Visualization Collaborator:

- Chandrajit Bajaj (Computer Science & ICES)